Title: Seasonal and comparative evidence of adaptive gene expression in mammalian brain size plasticity

Authors: William R. Thomas[1], Troy Richter[2], Erin T. O'Neil[2], Cecilia Baldoni[3,4], Angelique P. Corthals[5], Dominik von Elverfeldt[6], John Nieland[7], Dina K. N. Dechmann[3,4], Richard G. Hunter[2], Liliana M. Dávalos[1,8]

[1]Department of Ecology and Evolution, Stony Brook University, Stony Brook, New York, United States
[2]Department of Psychology, Developmental and Brain Sciences Program, University of Massachusetts Boston, Boston, Massachusetts, United States
[3]Max-Planck Institute for Animal Behavior, Radolfzell, Germany
[4]University of Konstanz, Konstanz, Germany
[5]John Jay College of Criminal Justice, New York, New York, United States
[6]Department of Radiology, University Medical Center Freiburg, Freiburg, Germany
[7]Health Science and Technology, Aalborg University, Aalborg, Denmark
[8]Consortium for Inter-Disciplinary Environmental Research, Stony Brook University, Stony Brook, New York, United States
*Correspondence: *William R. Thomas (william.thomas@stonybrook.edu)*

Abstract:
Contrasting almost all other mammalian wintering strategies, Eurasian common shrews, *Sorex araneus*, endure winter by shrinking their brain, skull, and most organs, only to then regrow to breeding size the following spring. How such tiny mammals achieve this unique brain size plasticity while maintaining activity through the winter remains unknown. To discover potential adaptations underlying this trait, we analyzed seasonal differential expression in the shrew hypothalamus, a brain region that both regulates metabolic homeostasis and drastically changes size and compared hypothalamus expression across species. We discovered seasonal variation in suites of genes involved in energy homeostasis and apoptosis, shrew-specific upregulation of genes involved in the development of the hypothalamic blood brain barrier and calcium signaling, as well as overlapping seasonal and comparative gene expression divergence in genes implicated in the development and progression of human neurological and metabolic disorders, including *CCDC22*, *FAM57B*, and *GPR3*. With high metabolic rates and facing harsh winter conditions, *Sorex araneus* have evolved both adaptive and plastic mechanisms to sense and regulate its energy budget. Many of these expression changes mirrored those identified in human neurological and metabolic disease, highlighting the interactions between metabolic homeostasis, brain size plasticity, and longevity.

Main Text

Introduction:

Typical mammalian brain development consists of unidirectional postnatal growth until reaching an adulthood maximum (*1*, *2*), but the Eurasian common shrew, *Sorex araneus*, seasonally changes the size of its body, most organs, skull, and —especially— its brain (*3–6*). In the most acute case of Dehnel's phenomenon (DP), or seasonal size plasticity, the common shrew first grows to an initial summer maximum as a juvenile, then reduces size in autumn losing up to 18% body mass, ~20% skull volume, and 26% brain mass, reaching its winter size minimum (*3–6*). Then, in the spring prior to mating, these shrews either partially or fully regrow these organs, reaching a second maximum. DP is hypothesized to be a plastic adaptation to decrease energy demand without slowing metabolism , improving shrew fitness during the low temperatures and limited food supply of winter (*3*, *4*, *6–12*). Corroborating this adaptive plasticity hypothesis, DP anticipates winter conditions and is both modulated by environmental temperature (*3*) and geographically variable (*4*). Although we have begun to reveal the molecular mechanisms of DP (*12*), the comparative context of proposed adaptations, and commonality of processes across brain regions remain unknown. Elucidating both the genetic basis and evolutionary mechanisms underlying DP will illuminate the adaptations involved in this unusual case of mammalian brain plasticity.

As a hypothesized wintering strategy, energy metabolism is key to the evolution of DP in *S. araneus* (*11*). Tiny mammals have limited options to survive winter conditions (*13*), and DP is exceedingly rare as a wintering strategy. While many mammals seasonally migrate away from low-temperature, low-productivity environments, some endure these conditions by reducing their energy requirements through hibernation; a phenotype that has independently evolved many times (*14–16*). The evolution and regulation of hibernation relies upon a suite of metabolic genes (*17*, *18*), including those associated with thermogenesis, circadian rhythms, and feeding behavior. Compared to most species, *S. araneus* has astronomically large energetic demands, with one the highest basal metabolic rates per unit of body mass identified in any mammal (*19*, *20*). To meet these energy requirements, *Sorex araneus* forage and feed constantly. Together with brief lifespans (~1 year) that nonetheless require surviving a single winter (*21*, *22*), these extreme metabolic demands constrain survival options for *S. araneus*. Thus, by decreasing resources devoted to energetically expensive tissue such as the brain (*23*), DP bypasses these constraints and expands the typical niche of a small mammal during winter while allowing this fast-living, predatory shrew to remain active year round.

Critical metabolic shifts have been implicated in the regulation of seasonal size plasticity at a molecular level (*10*, *12*, *24*). Previous stage-by-stage analyses of DP characterized gene expression and network topology in three regions of the body that undergo seasonal size change: both the cortex and hippocampus in the brain, and the metabolically active liver (*12*). While those analyses found decreased cholesterol efflux in the cortex and hippocampus during brain shrinkage, there were also profound metabolic changes across the body. Liver expression revealed reversible regulation of key metabolic transcription factors (*FOXO*s, *PPAR*s, *RXR*s), indicating a shift away from lipid- toward glucose metabolism during autumn shrinkage. Metabolomic data supported this pattern, and a potential internal circadian clock regulating metabolic changes was also identified. Together, those results indicated a brain-liver crosstalk is a pivotal avenue of communication to coordinate metabolic modifications underlying seasonal size change across organs. Although disruption of the brain-liver axis has been implicated in neurodegenerative diseases in other mammals (*25–28*), how a highly functional brain-liver crosstalk which coordinates the shrew's natural seasonal size change operates and evolved remains unknown.

We hypothesize DP, which involves metabolic shifts and inter-organ communication (*12*), has evolved through the combination of both physiological plasticity and genetic adaptation. This idea is twofold; phenotypic plasticity is not only adaptive in itself as the evolved spectrum of a trait, but can also allow populations of a species to persist in varying environments, leading to ancillary evolutionary adaptation

when given enough time and strength of selection (*29*). Thus, while temporal analysis of shrew expression can elucidate putatively adaptive plastic regulation, it will miss adaptive canalization of gene expression that has contributed to the evolution of DP. Therefore, plastic regulatory mechanisms and proposed adaptations can be further tested via cross-species comparisons of expression divergence. These cross-species comparisons treat expression as a trait and have been used to characterize diverse vertebrate adaptations including thermal tolerance and vision loss in fish (*30–32*), the effects of whole genome duplication on expression (*33–37*), sex specific alternative splicing in birds (*38*), and patterns of expression evolution in mammalian organs (*39–42*). By incorporating these comparative approaches with seasonally varying gene expression, we can further elucidate the role of plasticity and adaption in both the regulation and evolution of DP.

The hypothalamus is an intriguing candidate brain region for comparative analysis, as it is both the brain region with the most intense seasonal size change in shrews, and the center of bodily homeostatic maintenance across mammals. In shrews, the hypothalamus undergoes drastic seasonal size change, with a 31.6% volume reduction in autumn through winter, followed by a 47.8% increase in spring (*43*). As in a previous study (*12*), we analyze hypothalamic gene expression across size change and compare these molecular processes of brain size change to those identified in the hippocampus and cortex, such as decreased cholesterol efflux or parallels to neurological disease. However, across mammals, the hypothalamus plays a pivotal role in the maintenance of an energy budgets, with functions influencing: 1) energy intake and feeding behavior, 2) energy expenditure and metabolic rate, and 3) energy deficits and storage. While such functions are important for all mammals, these are critical for wintering mammals to maintain stable internal body temperatures as external temperatures decrease. For example, the hypothalamus can activate the sympathetic nervous system as temperatures decrease, stimulating thermogenesis in winter. Thus, shrews may deploy typical mammalian hypothalamic plasticity through DP. Alternatively, and considering how rare DP is, shrews may have evolved divergent approaches, akin to naked mole rat traits, where this species lives under consistent hypoxic conditions resulting in adaptations to decreased oxygen and blood flow across the brain (*44*). Comparative approaches, then, may be able identify novel adaptations that contribute to the evolution of DP in the shrew hypothalamus.

As the brain region able to quickly respond to change, the hypothalamus has remarkable plastic capabilities associated with metabolism (*45*), especially as environmental conditions vary between seasons and can be unpredictable. While the central nervous system (CNS) acts somewhat independently of bodily metabolism through the protective effects of the blood brain barrier (BBB), the CNS is still sensitive to bodily metabolic change. We hypothesize hypothalamic plasticity is central to the evolution and regulation of DP through both environmental sensing mechanisms and signaling responses to these stimuli. Specifically, we hypothesize adaptations in the shrew: 1) hypothalamic BBB associated with dynamic metabolic fluctuations, 2) sensing of metabolic state and seasonal size through hormonal signals, mediated by BBB-crossing of insulin, ghrelin, and leptin, and 3) responses to metabolic fluctuations involving ion-dependent signaling. With limited energy inertia, shrews must continuously sense their peripheral metabolism, and a combination of receptors and selective BBB permeability in the hypothalamus allows certain molecules to relay information from the peripherals to the brain. Among the best characterized of these are the peripheral hormones insulin, ghrelin, and leptin, the latter known to excite anorexigenic and inhibit orexigenic neurons in the arcuate nucleus of the hypothalamus. Finally, according to Ramon y Cajal's neuronal doctrine (*46*), differences in brain functional responses may stem from altered synaptic firing. Thus, inter- and intracellular ion concentrations play a large role in the communication between neuronal networks by propagating signals in response to perceived environmental stimuli.

To test these hypotheses, we analyzed both the seasonal and phylogenetic variation in shrew hypothalamic expression to detect signals of adaptive plasticity. First, we aimed to identify differential expression of genes across five stages of DP that might promote regulatory responses to seasonal

variation and can be functionally validated with cell line perturbations. Second, this analysis was paired with a comparative transcriptomics approach using hypothalamic expression data from 15 additional mammal species. These analyses infer adaptation by testing for branch-specific expression shifts using Ornstein-Uhlenbeck models. The objective of these evolutionary analyses was to quantify lineage-specific hypothalamic expression changes in *S. araneus*, with evolutionary expression divergence consistent with selection. Finally, by comparing individual genes and associated pathways from these two analyses, we can determine potential adaptive plasticity, indicating mechanisms that both potentially regulate DP and were selected for higher expression in the evolution of DP. Our expression results implicate several key processes in DP, including seasonal plasticity in feeding behavior, adaptive modulation of both hypothalamic blood brain barrier and downstream signaling, and plastic apoptosis responses.

Results

RNA sequencing, mapping, and quantification

Between and within species, measurements of RNA quality and alignment, quantification, and normalization procedures were suitable for analyzing differential evolutionary and temporal expression associated with DP (Supplemental Data). First, a single "hypothalamus" from our autumn data was removed, as the expression profile resembled that of a cortex sample. Thus, our novel shrew hypothalamus sequences (n=23) consisted of five summer juveniles, three autumn juveniles, five winter juveniles, five spring adults, and five summer adults. RNA extracted across these seasons had a mean RNA Integrity Number (RIN) of 6.6 (range 5-7.8) and a mapping rate mean of 50.8% (range 45.1-57.4%). Although four samples had lower than initially expected (<6) RIN values, mapping rate (an indicator of sequencing quality) was only slightly impacted and resembled previously published cortex (mean 53.7%; range 48.1-61.5%) and hippocampus (mean 54.0%; range 48.1-61.6%) data. For evolutionary analyses, hypothalamic RNA sequencing data sets were identified for 19 species comprising 5 mammal orders. Four species were removed from this experiment during filtration. *Oryctolagus cuniculus* and *Pan paniscus* were prepubescent, *Phodopus sungorus* was removed due to a low-quality genome assembly at the time of analysis, and *Papio anubis* was removed from this experiment because of its extremely low mapping percentage (mean 16.75%; range 9.5%-23.7%), which had a large effect on the count distribution. Remaining species had an average mapping rate of 56.4% (range 33.1-77.9%). Although RINs were not available for every species in the dataset, roughly similar mapping percentages suggest adequate RNA quality. Furthermore, normalization by library size should reduce potential biases from differences in mapping rate. We identified 6,496 single-copy orthologs found in all species with OrthoFinder and filtered normalized expression (TPMs) by these genes (oTPMs). Mean expression of orthologs across all species was 31.44 oTPM (range 20.66-44.91), with the shrew lineage having an average 39.42oTPM. The distributions of oTPM by species was visualized in Supplemental Figure 1, illustrating similar frequency distributions.

Temporal Expression

We identified several known neural signaling pathways correlated with patterns of seasonal hypothalamus expression that may be associated with changes during DP. We began by hierarchically clustering expression to identify patterns of gene expression through time. Most genes did not exhibit much variation through time, indicating constitutive gene expression in the hypothalamus, as only 786 of 19,296 genes passed our filters (>0.5-fold change between any two stages and 2 samples > 10 normalized reads). We identified 12 distinct clusters of gene expression patterns by bootstrapping (n=20) a gap statistic within cluster distances. Of these 12 clusters, five clusters consisting of 392 genes resembled a large divergence between summer juveniles and the remaining individuals (Supplemental Figure 2; Clusters 2, 3, 8, 11, 12). These genes likely represent a large developmental shift between recently postnatal shrews and the remainder of individuals, rather than a shift associated with seasonality or Dehnel's phenomenon. We then functionally characterized the remaining 394 genes (Figure 1A), which exhibited seasonal shifts, with a GO pathway enrichment using the DAVID Gene Functional Classification Tool. Although no enrichment pathway was significant after a Bonferroni correction, 14

pathways were enriched prior to correction ($p < 0.05$); with the five pathways with the lowest p-values including fluid shear stress and atherosclerosis, relaxin signaling, neuroactive ligand-receptor interaction, HIF-1 signaling, and PI3K-Akt signaling (Figure 1B). Many of these pathways have been implicated in various physiological processes, which suggests that variation identified in the hypothalamus are likely the result of autonomic processes in homeostatic maintenance.

We also discovered hundreds of differentially expressed genes between autumn (Stage 2) and spring (Stage 4) shrews that may mediate phenotypic divergence in both size (shrinkage vs. regrowth) and metabolic changes (liver expression shifts) associated with DP. By comparing the RNA expression of autumn and spring shrews, we found 333 differentially expressed genes, with 194 upregulated and 139 downregulated in spring (Figure 2A). Of these genes, 57 upregulated and 34 downregulated were differentially expressed to a higher degree (> absolute fold change 3). The hypothalamus had a similar number of differentially expressed genes during DP compared to previous experiments elucidating expression differences in the cortex (DEG=540) and hippocampus (DEG=266). We ran a GO pathway enrichment to functionally characterize the 333 DEGs in the hypothalamus and found only five pathways were enriched ($p<0.05$; Modified Fischer's Exact Test) with significant genes prior to multiple comparison correction. These pathways include four upregulated pathways; Fanconi anemia (9.3 fold-enrichment, $p<0.01$), GABAergic synapse (5.6 fold-enrichment, $p<0.05$), spliceosome (4.3 fold-enrichment, $p<0.05$), and nicotine addiction (9.42 fold-enrichment, $p<0.05$), with one downregulated pathway; apoptosis (5.6 fold-enrichment, $p<0.05$) (Figure 2B). The apoptosis pathway consists of significantly downregulated genes (from DESeq2 Wald test), *BCL2L1* (-0.5 Log-Fold Change [LFC] $p_{adj}<0.05$), *NGF* (-2.3 LFC, $p_{adj}<0.05$), *NFKB1A* (-2.3 LFC, $p_{adj}<0.05$), *FOS* (-1.7 LFC, $p_{adj}<0.05$), and *CTSK* (-1.2 LFC, $p_{adj}<0.05$), while the GABAergic pathways consists of upregulated *GABRE* (5.0 LFC, $p_{adj}<0.01$), *GABRQ* (4.4 LFC, $p_{adj}<0.05$), *CACNA1D* (0.6 LFC, $p_{adj}<0.05$), and *GNB3* (3.5 LFC $p_{adj}<0.05$) (Figure 2C). Differential expression for all genes can be found in Supplemental Data. Overall, the processes identified suggest regulation of cell death and synaptic plasticity in the hypothalamus may be associated with phenotypic changes during DP.

Cell Viability Analysis with BCL2L1 Overexpression

We examined the potential functional effects of apoptosis regulating gene, *BCL2L1*, which was differentially expressed between seasons, by propagating an *in vitro* model of domesticated ferret brain cells (MPF-CRL-1656, ATCC). We chose this cell line because there is no established cell line of *Sorex araneus*. *Mustela putorius furo* also undergoes a Dehnel's-like phenotype (*47*) and is more closely related to shrews than mice are. MPF cells were transfected with either the anti-apoptotic *BCL2L1* RNA or a scrambled version of *BCL2L1* (sBCL2L1) RNA. 24 hours after transfection, cells were exposed to heat stress followed by crystal violet staining. A significant difference in cell viability was observed between the heat scrambled compared to the control scrambled groups (df=3.56, $t_{3.56}=8.78$, $p<0.01$), however, there was no significant difference between cells transfected with *BCL2L1* compared to those transfected with sBCL2L1 when exposed to heat (df=3.37, $t_{3.37}=-0.99$, $p=0.39$).

Evolutionary Divergence in Expression

Analyses quantifying branch-specific shifts in expression identified hundreds of genes that were upregulated in the shrew hypothalamus compared to other mammals, suggesting adaptation for increased expression in these genes (Figure 3). EVE models found 222 genes significantly rejected ($p_{adj} < 0.05$) a single expression optimum for all species in favor of a second expression optimum for the shrew lineage. While nonsignificant genes had a mean 0.93-fold change, genes experiencing an expression branch-shift in shrews had a mean 9.66 oTPM fold change compared to the other species. To validate genes with expression branch-shifts as shrew-specific, we ran a dropout test for the shrew lineage, testing for phylogeny-wide evidence of selection for each gene. Of the 6,496 genes tested, 81 genes had significantly ($p_{adj} < 0.05$) lower β (within population variance to between species variance), suggesting selection

elsewhere in the phylogeny. None of these genes overlapped with those identified to be differentially expressed in the shrew, further validating the specificity of expression shifts.

We identified several changes associated with processes that may underlie DP. Pathway enrichment analysis identified two significantly enriched pathways: calcium signaling (2.8 fold-enrichment, $p<0.05$) and autophagy (9.1 fold-enrichment, $p<0.05$) (Figure 3). Upon manual inspection of the list, we also identified several other potential adaptive processes, including blood-brain-barrier formation and function, feeding behavior and leptin responses, metabolism, neuroprotection, and GABAergic neuron development (Figure 3, Table 1).

Many of these putative adaptations mediate responses to environmental cues centered around energy demands. Five of the genes experiencing branch-shift changes in expression were also differentially expressed between autumn and spring individuals, suggesting not only an adaptive shift in the shrew lineage associated with the evolution of Dehnel's phenomenon, but also a direct molecular mechanism for brain changes. The five genes that overlap between both analyses include (Figure 4): *CCDC22*, which plays an important role in endosomal recycling of membrane proteins (*48*); *FAM57B*, which mediates synaptic cell membrane architecture and function (*49*), *GPR3*, an orphan G protein-coupled receptor linked to both Alzheimer's disease (*50*) and obesity (*51*); *LMX1A*, a transcription factor essential for dopaminergic neuron development (*52*); and *PAQR4*, which appears to regulate growth and apoptosis through sphingolipid synthesis in human cancers (*53*).

Discussion

By characterizing both seasonal and between-species differential expression of the hypothalamus, we generated and probed a unique data set, discovering expression shifts associated with extreme brain size change in *Sorex araneus*. While the focus on seasonal hypothalamus expression provides insights into both metabolic regulation and processes underlying brain size change, evolutionary shifts in expression can reveal the underpinnings of mammalian brain degeneration and regeneration in a natural system. Our analyses identified a suite of genes related to energy homeostasis that were both seasonally plastic and adaptively upregulated in the shrew, reinforcing the role of metabolism in both the evolution and regulation of DP. We also found shrew-specific upregulation of genes associated with the development of the hypothalamic blood brain barrier, which we hypothesize improves the metabolic sensing capabilities of the hypothalamus, further highlighting the importance of brain-liver crosstalk in promoting seasonal size change (*12*). Other molecular mechanisms, including adaptive calcium signaling and plastic apoptotic responses, were also implicated in DP. Many of these results, including genes that were both seasonally plastic and evolutionarily upregulated, resemble expression changes found in human neurological and metabolic disease, and thus may prove important for therapeutic treatment of those diseases.

Plastic Adaptations of Metabolism, Feeding Behavior, and Leptin Responses

Seasonal expression variation in the shrew hypothalamus was largely associated with the maintenance of homeostasis, especially processes related to energy balance, corroborating the metabolic hypothesis of DP evolution in the shrew. Although DP has been proposed to reduce shrew energy requirements by limiting energy devoted to the maintenance of larger tissues (*4*, *7*, *20*), the extent of system-wide metabolic shifts during shrinkage and regrowth, particularly in the liver, has only recently been revealed (*12*). We found three pathways enriched for genes with seasonal variation in the hypothalamus which also have metabolic associations: relaxin signaling, phosphoinositide-3 kinase (PI3K) signaling, and neuron ligand receptor interactions. Relaxin, a neuropeptide, plays a pivotal role in many physiological functions in model organisms, including food and water intake (*54–57*); food restriction upregulates relaxin-3 (*RLN3*) *in vivo* (*58*), while administering RLN3 protein into the rat hypothalamus vastly increases food intake (*59–62*). Relaxin has also been found to activate the PI3K pathway (*63*, *64*), which mediates feeding behavior and glucose homeostasis (*65–69*), as well as angiogenesis via vascular endothelial growth factor (VEGF) production (*64*, *70*, *71*). PI3Ks activity influences feeding behavior and weight gain in response to key

metabolic hormones, including leptin and insulin (*67–69*, *72*). Lastly, the neuroactive ligand-receptor interaction pathway, a subclass of KEGG Environmental Information Processing pathway, is associated with responses in model organisms to shifts in diet (*73*), stress (*74*), and temperature (*75*, *76*), all of which the shrew experiences during seasonal changes. Although exploration of gene function in *S. araneus* has only begun, seasonal expression in the hypothalamus indicates maintenance of metabolic homeostasis, likely reflecting an extreme physiology that pairs disproportionately high metabolic rates (*20*) with lifespans shorter than expected by body size (~1 year) (*21*, *22*). Facing scarcity in the winter, yet maintaining costly activity in their environment, shrews must efficiently regulate feeding behavior, food intake, and energy homeostasis, and we find signatures of such regulation in their hypothalami.

We also found evidence for adaptive expression relating to maintenance of energy balance, specifically in feeding behavior and leptin responses, further emphasizing the importance of selection to meet high energetic demands in wintering environments in the evolution of DP. Key genes associated with the hypothalamic leptin response, such as *NPY*, *AgRP*, or *POMC*, were not universally orthologous and so could not be analyzed, but there was evolutionary upregulation of many genes involved in downstream leptin responses (*FOXO4*, *GRB2*, *IRX5*, *AGT*) (Figure 3, Table 1). Unlike their upstream effectors, these genes may have subtle effects on continuous feeding behavior. In the hypothalamus, FOXO1 negatively regulates POMC and promotes AgRP expression (*77*), which can contribute to leptin resistance resulting in a long term appetite suppression (*78–80*). However, much less is known about the hypothalamic functions of the *FOXO1* paralog, *FOXO4*. In mouse adipocytes, leptin- dependent expression of *FOXO4* can rapidly clear blood glucose levels (*81*), which can lead to energy storage and decreased satiety. We hypothesize that, in shrews, upregulation of *FOXO4* could either increase blood glucose clearance or leptin resistance, reducing long term satiation and promoting continuous feeding. Further supporting this hypothesis, we also found shrew-specific upregulation of other genes associated with leptin sensitivity, such as *GRB2*, which in hamsters regulates seasonal leptin sensitivity and body weight (*82*), and *IRX5*, whose mice knockouts exhibit decreased weight and food intake due to an enhanced hypothalamic leptin response (*83*, *84*). Functionally, evolutionary upregulation of these genes in the shrew hypothalamus may result in evolved leptin insensitivity, instead of the development of leptin resistance. Reduced leptin sensitivity in shrews could reduce overall satiation, promoting foraging even when the short-term energy budget is balanced thereby improving anticipatory storage before winter.

Evolution of BBB Permeability and Energy Sensing

Comparative analyses also indicate shrews may have evolved adaptive environmental sensing. We found upregulation of several proangiogenic genes associated with the formation and function of the blood brain barrier, including *VEGFA* and *WNT7A*. In normal neural development, neural progenitor cells and surrounding astro- and pericytes express these two genes defining an expression gradient that guides blood vessels to form the blood brain barrier (*85–87*).

While this suggests *VEGFA* and *WNT7A* upregulation in the shrew may increase vascularization of the brain, continued expression of *VEGFA* beyond development increases BBB permeability, leading to a breakdown of its protective effects (*88*, *89*). BBB permeability is a common symptom of many disease-like states including neuroinflammation (*90*) and neurodegeneration (*90–92*). The hypothalamus BBB consists of tanycytes and highly fenestrated capillaries with less tight junctions (*93*), replacing the less permeable BBB of other brain regions with a specialized barrier that improves nutrient and energy sensing through dynamic passage of molecules from peripheral circulation (*94–96*). Experiments on mice indicate reduced blood glucose levels from fasting promote capillary fenestration in the hypothalamic BBB via upregulation of *VEGFA*, eliciting feeding responses through increased hypothalamic exposure to glucose levels (*94*). In shrews, adaptive upregulation of *VEGFA* and *WNT7A* may constitutively increase capillary fenestration, an adaptation of the BBB to improve hypothalamus metabolic sensing and signaling in response to high energy demands. Notably, adaptive expression of *VEGFA* has also been identified in the seasonal vascular plasticity of other mammal species, including reproductive sheep (*97*,

98), bison (*99*), and squirrels (*100*). Reproduction is an extremely metabolically demanding process, thus, constitutive shrew specific upregulation of *VEGFA* to meet unusually high metabolic demands may parallel mechanisms used in seasonal reproduction.

Calcium Signaling and Apoptosis

Calcium signaling is a ubiquitous form of neural communication (*101*, *102*) that occurs through the regulation of intra and extracellular calcium concentrations, transmitting signals that can release neurotransmitters (*103*, *104*) and promote gene expression (*105–108*). Thus, it has been implicated in numerous functions including dendrite growth (*109*, *110*), synaptogenesis (*111–113*), and initiation and maintenance of long-term potentiation (*114*, *115*). In shrews, adaptive calcium signaling through the upregulation of several calcium-responsive genes (*VEGFA*, *CASQ1*, *HRH2*, *TACR2*, *PPIF*, *SPHK2*, *GRIN1*) may improve environmental information relay in the hypothalamus, both internally and throughout the central nervous system.

We found that *HRH2* is upregulated in the hypothalamus of shrews, while maintaining strong sequence homology with other mammals. Although adaptive calcium signaling could have numerous physiological effects associated with shrew fitness or DP, many neuroadaptations (*116*, *117*) have pinpointed the effects of calcium signaling by identifying the local functions of calcium responsive molecules and genes (*118*, *119*). One such neuroadaptation involves the histamine receptor HRH2, which depresses neuronal action potential when bound to histamine by blocking calcium-dependent potassium channels (*120*, *121*). In the hypothalamus, HRH2 and other histamine receptors regulate circadian rhythms and feeding behavior (*122*). Alternatively, agonism of HRH1 in rodents, an excitatory receptor in contrast to HRH2 (*123*), reduces food consumption by ~50% (*124*), while a genetic knockout of *HRH1* both increases feeding and disrupts circadian feeding behavior (*125*). Data on *HRH2* are sparse in comparison to those on *HRH1* (*126*), but agonism of HRH2 did not significantly affect rodent feeding behavior (*124*) and mice *HRH2* knockouts reduce nocturnal mice activity (*126*). We propose the ~12-fold upregulation of *HRH2* receptors in shrews, despite being evolutionary divergent from rodents, also disrupts light entrainment, with the potential to increase food intake.

Calcium signaling also regulates opposing processes, including both cell survival and programmed cell death (*118*), and thus evolutionary upregulation of genes involved in these processes may be associated with seasonal brain shrinkage and regrowth. Autophagy is the degradation of cellular parts to provide energy and materials to maintain cellular homeostasis under stressful conditions. We found an evolutionary upregulation of autophagy genes in the shrew hypothalamus, including *MLST8*, an integral component of the mTOR protein complex 1 (mTORC1), which regulates sugar and lipid metabolism(*127*), but also has recently been found to modulate autophagy in response to nutrient deprivation (*128*). However, sensing calcium levels is also vital for the regulation of apoptosis and efflux of damaged or dying cells. Two evolutionarily upregulated genes *PPIF* and *SPHK2*, can promote apoptosis associated with mitochondrial calcium influx. PPIF is an important component of the mitochondrial permeability transition, which responds to cellular calcium overload and oxidative stress by promoting cell death (*129–132*). Similar to *PPIF*, overexpression of *SPHK2* in stressed cells induces cell cycle arrest and promotes apoptosis through a series of signaling cascades that increase cytosolic calcium and promote the release of pro-apoptotic cytochrome C from the mitochondria (*133*, *134*). While both *SPHK2* and *PPIF* are overexpressed and likely contribute to neuronal death in both human patients with Huntington's or Alzheimer's disease and rodent models of these diseases, knockout or inhibition of these genes protects against neurodegeneration (*135–138*). In the shrew hypothalamus, canalized upregulation of these genes likely influences cell survival and death, but precisely how requires further investigation.

Validating the critical role of apoptosis regulation in Dehnel's phenomenon, several apoptosis-regulating genes are differentially expressed between seasons. We found apoptosis pathway genes, including *NGF*, *NFKBIA*, and *BCL2L1*, are all upregulated during shrinkage and downregulated in regrowth, despite

previous analyses that identified no changes in brain cell numbers in most brain regions through DP (*139*). Regulation of apoptosis may represent a convergent mechanism across wintering strategies, as natural experiments found seasonal reduction of apoptosis, including upregulation of BCL2L1, occurs in various organs of hibernators (*140*, *141*), including the brain (*142*). Specific to DP, this result indicates tight regulation of cell survival during brain size changes and periods of metabolic and environmental stress: a balance between brain shrinkage and maintenance of cell numbers.

Preserving cell numbers despite size change requires both pro- and anti-apoptotic regulation. Known functions of genes cycling during DP bolster this view: NGF is an upstream activator of neuronal cell death through interactions with the p75 neurotrophin "death" receptor (*143*), but NGF can promote cell survival by activating the NFKB pathway that blocks apoptosis further downstream (*144–146*). For example, in primary rat hippocampal neurons, NGF promotes expression of anti-apoptotic *BCL2L1* through an NFKB-dependent pathway (*147*) whose upregulation reduces apoptosis and promotes cell survival in rodents (*148*, *149*). To test if autumn upregulation of these genes acts to reduce apoptosis, we overexpressed *BCL2L1* in a related mammalian neural cell line, but we did not find a rescue against apoptosis from heat. This result defied our expectations, with several possible explanations. Methodologically, heat-induced apoptosis may not accurately reflect the challenges to cell survival present in DP. Alternatively, the anti-apoptotic function of *BCL2L1* may be specific to the unique neural environment of shrews, with apoptosis being propagated through alternative pathways or species- specific gene interactions. DP-related apoptosis regulation as an adaptation may be convergent across wintering mammals, but the regulatory mechanisms of this process through shrew size change require further investigation.

Disease-associated Adaptive Plasticity

A subset of genes, *CCDC22*, *FAM57B*, *GPR3*, *LMX1A*, and *PAQR4*, are both seasonally plastic and evolutionarily upregulated in the shrew hypothalamus (Figure 4). The combination of seasonal and evolutionary upregulation suggests these genes play integral roles in DP, likely through adaptive plasticity. Many of these genes are directly related to the development and progression of neurological disorders in humans. While some of these genes may modulate DP, others may be a byproduct of brain size change, or act as neuroprotection against the negative consequences of brain size and structure changes.

CCDC22

CCDC22 regulation in shrews may provide protection against harm incurred during seasonal size changes. The coiled-coil domain containing 22 protein (CCDC22) plays a key role in endosomal recycling of proteins and is a novel candidate gene for several neurological disorders. CCDC22 is a subunit of the CCC (CCDC22, CCDC93, COMMD) complex that aids in trafficking and recycling of endosomal membrane proteins (*48*, *150*, *151*). Improper recycling and resulting protein aggregation readily occurs in neurons, as they do not proliferate (*152*, *153*), and has also been implicated in neurodegenerative diseases, including cytotoxicity in amyotrophic lateral sclerosis (*154*), amyloid-B aggregation in Alzheimer's disease (*155–157*), and MUL1 degradation in Parkinson's disease (*158*). Missense mutations and subsequent downregulation of CCDC22, are potential mechanisms underlying X-linked intellectual disability (*159*, *160*) and Ritscher-Schinzel syndrome (*160–162*) in humans. Both disorders are characterized by macrocephaly, malformations of the brain, craniofacial abnormalities, and intellectual disabilities. In pubescent spring shrews, we found CCDC22 has a ~7-fold upregulation compared to other mammals. This evolutionary upregulation may protect against neurodegeneration, as brain size and structure are altered during seasonal cycling. We also found a significant upregulation during spring compared to autumn shrinkage. Neuroprotective functions may be especially important in spring, as brain mass returns increasing the need for endosomal recycling of proteins and may explain seasonal plasticity in CCDC22 expression in tandem with adaptive upregulation.

FAM57B

Combined evolutionary upregulation and seasonal plasticity was also found in the expression of *family with sequence similarity 57 member b* gene, *FAM57B*, which has been associated with 16p11.2 deletion syndrome (*163*). This deletion leads to copy number variations and haploinsufficiency of 25 genes, including *FAM57B* (*164*), resulting in autism spectrum disorders (*165*). Disease models of this deletion have a variety of symptoms that parallel both shrew ecology and DP. In rodents, heterozygous 16p11.2 deletion leads to hyperactivity, craniofacial defects, reduced brain size, and altered brain morphology and shape (*163*, *166*, *167*), with duplications showing the opposite effects on weight, activity, and craniofacial morphology (*166*, *167*). *FAM57B* haploinsufficiency in the more evolutionarily divergent zebrafish creates similarly substantively modified phenotypes, with heterozygous and homozygous knockouts of *FAM57B* resulting in abnormal axon development (*168*) and increased head and body size (*164*, *167*). Brain and body phenotypes related to *FAM57B* expression may be associated with the gene's role in lipid metabolism and synaptic composition (*169*, *170*). Across animals, the dosage and compensation effects of *FAM57B* expression have conserved impacts on metabolism, behavior, brain size, and body size. In the shrews, *FAM57B* has a higher baseline expression than in model organisms. We hypothesize upregulation of *FAM57B* in shrews contributes to seasonal plasticity of the skull, brain and body.

GPR3

As with *CCDC22* and *FAM57B*, G-protein receptor 3, GPR3, influences both metabolism and neural development, but unlike them, its effects are age dependent. In mouse models of apoptosis, *GPR3* has been associated with neurite outgrowth and maturation by promoting neuronal survival pathways (*171*). Despite these benefits, overexpression of *GPR3* also been implicated in Alzheimer's disease and contributes to amyloid beta generation (*50*, *172*). The metabolic effects of *GPR3* also indicate age-dependent benefits and outcomes. *GPR3* knockout mice exhibit late-onset obesity associated with reduced adipose thermogenesis (*51*). If the benefits of *GPR3* are age dependent, downregulation of this gene during brain regrowth in the shrew may be neuroprotective. Although evolutionary upregulation may increase neuronal cell survival during size change, plastic regulation is also important to reduce its negative consequences as shrews age. We propose *GPR3* expression likely influences the adaptive and plastic processes important in DP, including apoptosis/cell survival, calcium signaling, and metabolism.

Conclusion

We discovered evidence for adaptive evolution of gene expression involved in the regulation of metabolism, cell survival, and size plasticity associated with DP. Not only does the hypothalamus shrink to reduce energetic load during winter, but it must also control metabolic homeostasis during these changes. Our results reveal numerous conserved and novel gene expression mechanisms that likely underlie the central functions of the hypothalamus during DP. While previous work had hinted at the metabolic nature of DP, by pairing seasonal differential expression with comparisons to other species, we identified adaptations likely involved in the evolution of this unique brain size plasticity. Metabolism, body size, and longevity are intrinsically linked life history factors. In the shrew, unusually high metabolic rates force winter activity, leading to intense metabolic sensing and regulation and changes in cell survival pathways, and –through both the evolution of DP and these sensing and regulatory adaptations– shortened lifespans. Together, these gene expression adaptations both likely underlie drastic seasonal size change and mitigate its detrimental effects.

Materials and Methods

Shrew Sample Collection

We used tissues from shrews collected for experiments analyzing gene expression and metabolic shifts in brain regions through DP (*12*). Briefly, S. *araneus* were collected from a single German population (47.9684N, 8.9761 E) across five different stages of DP from June 2020-June 2021 (n=25, n_{per_stage} = 4-5). Shrews were trapped with insulated wooden traps that contained mealworms, which were checked every two hours. This protocol was used to minimize trap-related stress from heat/cold shock or lack of food

and thus reduce stress-related variation on gene expression. Shrews were then euthanized via vascular perfusion of PAXgene Tissue Fixative. Brain regions were dissected into individual regions in cold fixative and then incubated in PAXgene Tissue Stabilizer for 2-24 hours before long-term storage. Samples were preserved in stabilizer at -180°C in liquid nitrogen until RNA extraction.

RNA Extraction, Library Preparation, and Sequencing

We extracted the *S. araneus* hypothalamus and olfactory bulb using the same methods described for the cortex and hippocampus in previous work (*12*). These extractions reduce degradation due to heat and improve RIN from standard Qiagen Micro RNAeasy protocols by disrupting tissue on dry ice using glass, instead of plastic, mortar and pestles. A full list of changes to the Qiagen Micro RNAeasy protocol can be found in our previous manuscript (*12*). RNA was sent to Azenta Life Sciences for quality control (nanodrop and RNA ScreenTape), library preparation, and sequencing. Hypothalamus libraries were prepared with poly-A selection and sequenced for approximately 15-25 million reads per sample in 150bp PE reads.

RNA sequences from other species were collected from the NIH National Center for Biotechnology Information's (NCBI) Sequence Read Archive data sets. First, we searched the Sequencing Read Archives (SRA) for the keyword hypothalamus, filtered by both RNA and mammal species. As models described below rely on using the variance both between and within species, species required three or more biological samples to be included. This removed any species that had only one hypothalamus sample sequenced. Species were excluded from the study if a genome assembly was not readily available, as this information was needed for an unbiased alignment of reads. Our final criterion was to only include species for which post-pubescent individuals were available to reduce noise from age effects and the onset of puberty. If the onset of puberty was not specifically stated for the dataset, AnAge was used to determine if samples were pubescent. For the remaining species, if multiple hypothalamus RNA-seq data sets were available, we used less stringent rules to determine which data to select. First, to reduce domestication or captivity effects, we chose wild or non-domesticated individuals over laboratory-raised animals. Second, to reduce the variance from different extraction protocols and sequencing methods, we used samples from the same experiments or larger data sets, available for multiple species or brain regions. Using samples from datasets with multiple regions or species also suggests intimate knowledge of neural anatomy, increasing confidence in dissections. Third, we used a maximum of eight samples per species and attempted to maintain a 1:1 sex ratio when possible. We did not filter by sequencing method (e.g., used 50bp SE as well as 150 PE reads) or sequencing depth, as filtering poor reads and normalizing for library depth and content should account for both these factors.

RNA Quantification, Normalization, and Orthology

Adapter sequences were trimmed from the raw reads using the default parameters of fastp (*173*), which is able to autodetect adapters regardless of different library preparations across species. This program also corrected and pruned low quality bases and reads using a sliding window approach. Processed reads were aligned and quantified with Kallisto 0.46.2 (*174*), which probabilistically estimates gene counts through pseudo-alignment to each species-specific genome assembly. Samples were removed from the data set if mapping rate was below 30%, indicating either poor sequencing or low assembly quality. Additionally, novel shrew hypothalamus sequences were compared against previously published shrew region data to verify tissue type. Gene counts for all species were then normalized for total library size into Transcripts Per Million (TPM). Orthologous genes between species were inferred with OrthoFinder (*175*) using default parameters, retaining only single-copy orthologs identified across all species. Visualizations of the frequency distribution of the orthologous (oTPMs; Supplemental Figure 1) were used to identify outlier species.

Branch-shift Changes in Expression

We modeled gene expression as a trait using phylogenetic comparative methods, as these account for evolutionary divergence among species (*176*). We ran Expression Variance and Evolution models (EVE) to test for significant changes of expression in the shrew lineage (*39*). EVE models both parameterize and estimate the ratio (β) of population (within species) to evolutionary (between species) variance, such that high β ratios indicate expression plasticity, and low β ratios indicate differential expression between species, necessary for inferring selection. We ran two EVE models to test for divergence in expression in the shrew lineage. First, we tested for branch-specific expression level shifts by contrasting the likelihood of two Ornstein-Uhlenbeck models for the data, one with a single expression optimum (null; stabilizing selection), and another with a second optimum on the shrew branch (selection). A likelihood ratio test between the null and selective hypotheses for each gene (χ_1^2) was conducted using these likelihoods. A Bonferroni correction was used to account for multiple hypothesis tests to identify candidate genes under selection (p_{adj}<.05). For the second model, we ran a dropout test to further validate the specificity of the expression change in the shrew lineage. After removing the shrew expression data, we identified genes with high expression divergence across the phylogeny (significantly low β ratios), which would indicate relaxed or diversifying selection. This gene list was compared to that from first model to prune genes not specifically associated with divergence in the shrew. Both models described above ran on the Bayesian molecular-clock mammalian phylogeny of (*177*) pruned to match our species sample. Finally, we used the DAVID functional annotation tool (*178*) to determine enriched KEGG Gene Ontology (GO) pathways from the candidate gene set.

Temporal Clustering

To analyze the temporal variation of shrew expression in the hypothalamus, we temporally clustered our data using the package TCseq (*179*). We began by further normalizing our data across DP stages using the median of ratios from DESeq2 (*180*), which normalized for library size and content. Genes with consistent expression across time with little variation between stages would not be associated with observed phenotypic changes. These genes were filtered from this data set by only selecting genes with an absolute fold change of 0.5 between any two stages. We also removed genes with low expression that would appear to have high fold changes despite lacking enough transcript expression to influence phenotype, retaining only reads with two samples > 10 normalized reads. After filtering, counts for each stage were converted to mean z-scores and then clustered into groups of similar gene expression profiles using fuzzy cmeans clustering. The number of resulting gene clusters was calculated a priori, by bootstrapping (n=20) a gap statistic that minimizes within-cluster distances. Genes with highest membership in clusters associated with variation across all stages (seasonal effect; Clusters 1, 4, 5, 6, 7, 9, 10), as compared to those that just show divergent expression in Stage 1 (developmental effect; Clusters 2, 3, 8, 11, 12), were analyzed for KEGG GO enrichment using DAVID functional annotation (*178*).

Differential Gene Expression

We tested for differential gene expression between autumn (Stage 2) and spring (Stage 4) individuals, as these seasons differ in hypothalamic size phenotype (shrinkage vs. regrowth) (*43*), and were previously identified divergence in liver expression related to metabolism (*12*). To test for significant differential expression, we fit a negative binomial generalized linear model to the normalized (median of ratios) gene counts using DESeq2 (*180*). We then tested for significant differences in gene expression between autumn and spring using a Wald test, followed by multiple testing correction on resulting p-values with the Benjamini and Hochberg procedure (*181*). Significantly differentially expressed genes were binned by fold change (>1.58 log-fold change), to quantify differentially expressed genes of high effect. Significant differentially expressed genes were also used to identify KEGG GO enrichment (*178*), and compared against the candidate list of genes with branch shift changes in expression to identify genes both plastic across seasons and consistent with expression adaptation in the shrew.

Cell culture

Mustelo putoris furo (MPF) brain cells (ATCC, CRL-1656) were cultured in 10mL of Basal Medium Eagle (BME) supplemented with 14% sheep serum. Cells were cultured in 60.8-cm^2 treated tissue culture dishes at 37°C in 5% CO_2 atmosphere and 95% humidity. With induced cell death, cells were seeded into treated flat bottom six-well plates with 2mL/well of complete culture media.

Cell death induction

Three experiments were conducted to induce cell death in MPF cells (cold induced, peroxide induced, and heat induced), with only heat causing significant decrease in cell viability. *Cold induced*: Two 60.8-cm^2 tissue culture dishes of MPF cells were seeded into two six-well plates for 24 hours before reaching 80% confluency. In one experiment, "short cold" apoptosis was performed by immersing the six-well plate into a 0°C ice-water bath for 2 hours, followed by 3 hours of rewarming to 37°C in an incubator. Cells were then treated with crystal violet staining. In a similar experiment, "long cold" apoptosis was performed by immersing the six-well plate into a 0°C water bath for 4 hours, followed by 24 hours of rewarming to 37°C before crystal violet staining. *Peroxide-induced cell death*: Two 60.8-cm^2 tissue culture dishes of MPF cells were seeded into two six-well plates for 24 hours before reaching 80% confluency. Hydrogen peroxide (H_2O_2) induced cell death was performed by treating the plate with 125µM H_2O_2 followed by 3 hours of incubation at 37°C. Cells were then treated with crystal violet staining. *Heat-induced cell death*: Two 60.8-cm^2 tissue culture dishes of MPF cells were seeded into two six-well plates for 24 hours before reaching 80% confluency. Heat cell death was attempted by immersing the six-well plate into a 45°C water bath for 2 hours, followed by re-cooling to 37°C prior to crystal violet staining.

In vitro transcription and transfection of cells

The AmpliScribe T7 High Yield Transcription kit (Lucigen) was used for RNA in vitro transcription with a 2-hour incubation at 37°C using gblock sequences available in supplemental. Sequences were designed with a T7 promoter inserted at the beginning to facilitate transcription (Integrated DNA Technologies). RNA transcripts were purified using the Qiagen miRNA kit and concentration determined using a Nanodrop2000 (Thermo Fisher Scientific). Two 60.8-cm^2 tissue culture dishes of MPF cells were seeded into two six-well plates for 24 hours before reaching 80% confluency. 300ng of *BCL2L1* RNA or a scrambled form of *BCL2L1* RNA were transfected with Lipofectamine 3000 into each well for 24 hours according to manufacturer's instructions (Thermo Fisher Scientific). In short, two tubes were used to make a master mix for each RNA sample. Tube 1 contained 125µL/well of Opti-mem (Thermo Fisher Scientific) with 7.5 µL/well of Lipo3000. Tube 2 contained 125µL/well of Opti-mem, 5µL/well of P3000 and 300ng/well of RNA. Tube 2 was added to tube 1 and incubated 15 minutes at room temperature. The solution was then gently mixed and dispersed evenly to cells.

Crystal violet cell viability assays

Crystal violet solution was made using 500mg crystal violet powder in 100mL of 50% methanol. Cells were cultured to 80% confluency in two six-well plates. Complete media was aspirated in wells and washed three times in 1mL of 1X DPBS before 500µL of crystal violet solution was added to each well. Plates were wrapped in foil and placed on a shaker for 30 minutes. After time elapsed, crystal violet was removed, and cells were washed with tap water until free color was no longer visible. Plates were left at room temperature for 10-15 minutes until dry. 500µL of 100% methanol was added to each well and plates were put on a shaker for one hour at room temperature. 100µL of solution was taken from each well in triplicate and added to a 96-well plate. 100µL of 100% methanol was added in triplicate to a row for normalization of background absorbance. Wells were read at 570nm using a spectrophotometer (BioTek). For viability, data are reported as a percentage of control or optical density for absorbance. For statistical analysis, differences were judged to be statistically significant when $p<0.05$ by a Welch's two sample t-test.

Data Availability

Supplementary tables, data, results, and code deposited and found on Github https://github.com/wrthomas315/Sorex_Hypothalamus_Transcriptomics. Raw sequencing data located in the NCBI Sequencing Read Archive (BioProject PRJNA941271). Supplemental Figures. S1–S2: DOI: https://doi.org/10.6084/m9.figshare.26049739.v1.

Grants

Human Frontiers of Science Program, award: RGP0013/2019 (to Dina K. N. Dechmann, John Nieland, Liliana M. Dávalos).

WRT was supported in part by a Stony Brook University Presidential Innovation and Excellence award to LMD.

Disclosures

Authors declare no competing interests.

Author Contributions

Conceptualization: DD RGH WRT
Methodology: ETO LMD RGH TAR WRT
Software: WRT
Validation: APC ETO
Formal analysis: APC ETO TAR WRT
Investigation: CB ETO TAR WRT
Resources: CB DD ETO RGH TAR
Data Curation: WRT
Writing – Original Draft: ETO TAR WRT
Writing – Review and Editing: APC CB DD DE ETO JDN LMD TAR
Visualization: ETO TAR WRT
Supervision: LMD RGH
Project administration: DD LMD
Funding acquisition: APC DD LMD JDN

Figure Legends

Figure 1 – (A) Hierarchical clustering of expression identified 12 distinct clusters, of which seven clusters (1, 4, 5, 6, 7, 9, 10) comprising of 394 genes, showed variation consistent with seasonality or Dehnel's phenomenon. **(B)** Functional characterization of these genes using KEGG GO pathways found an enrichment of 14 pathways ($p<0.05$), many of which have been implicated in hypothalamic control of homeostatic maintenance, including, relaxin signaling, neuroactive ligand-receptor interaction, HIF-1 signaling, and PI3K-Akt signaling.

Figure 2 – (A) Volcano plot of significant ($p_{adj}<0.05$) differentially expressed genes (colored) between phenotypic extremes of hypothalami size change (Stage 4 vs Stage 2) plotted by log fold-change. Vertical thresholds represent a 1.58 log fold-change in expression of (high effect; dark colors). **(B)** Pathway enrichment analysis identified 5 pathways to be enriched for differentially expressed genes: apoptosis (downregulated), spliceosome, Fanconi anemia, GABAergic synapse, and nicotine addiction (upregulated). **(C)** Patterning of gene expression across stages of Dehnel's phenomenon for genes found in the apoptosis pathway (*BCL2L1*, *CTSK*, *FOS*, *NFKBIA*, *NGF*) and those associated with GABAergic synapses (*CACNA1D*, *GABRE*, *GABRQ*, *GNB3*). **(D)** Cell viability of *Mustela putorious furo* neural cell lines exposed to four treatments: scrambled *BCL2L1* overexpression, *BCL2L1* overexpression, heat with scrambled BCL2L1 overexpression, and heat with *BCL2L1* overexpression. Heat significantly reduced the cell viability compared to controls but was not rescued by *BCL2L1* overexpression.

Figure 3 – (A) Heatmap and boxplots of genes with shrew-specific upregulation compared to other mammals associated with processes including calcium signaling, neurological functions, **(B)** blood brain barrier plasticity, and **(C)** food intake and leptin response.

Figure 4 - Boxplots of genes (CCDC22, FAM57B, GPR3) showing both evolutionary upregulation (**A**) in the shrew and differential expression between Stage 4 and Stage 2 individuals (**B**), which are implicated in the development and progression of human neurological and metabolic disorders.

Tables

Table 1 – Significant shrew-specific upregulation of genes associated with calcium signaling pathways, blood brain barrier plasticity, food intake and leptin response, and other related functions.

Gene	Function	FC	P-value	KEGG (p<0.05)
WNT7A	BBB/Neurogenesis/Angiogenesis	8.60	0.000	NA
MFSD2A	Transports DHA across blood brain barrier/Fasting induced	5.22	0.000	NA
SLC22A23	BBB plasticity	4.69	0.000	NA
VEGFA	BBB plasticity/Calcium Signaling	4.04	0.024	Calcium Signaling
CASQ1	Calcium Signaling/myopathy	7.22	0.000	Calcium Signaling
HRH2	Calcium Signaling/Sleep related/Histaminergic neurons	11.74	0.000	Calcium Signaling
TACR2	Calcium Signaling	14.21	0.000	Calcium Signaling
PPIF	Calcium Signaling	4.92	0.000	Calcium Signaling
SPHK2	Calcium Signaling/Food intake	3.18	0.025	Calcium Signaling
GRIN1	Calcium Signaling/Food intake	3.60	0.016	Calcium Signaling
FOXA2	Food intake	19.37	0.000	NA
SDC1	Food intake	10.74	0.000	NA
AGT	Leptin Response/Food Intake/FOXO1	4.23	0.029	NA
IRX5	Leptin response/Food intake/Neurogenesis	3.83	0.006	NA
GRB2	Leptin Response	3.36	0.003	NA
FOXO4	Leptin Response	5.99	0.000	NA
GPR3	Thermogenesis/Obesity	3.77	0.002	NA
KCNJ10	Metabolic homeostasis/Tanycyte formation	4.87	0.002	NA
ELOVL2	Lipid Metabolism/Elongation of VLFA	6.29	0.001	NA
MRPS6	Mitochondria protein synthesis/Parkinson's	4.00	0.000	NA
ATG101	Autophagy	3.95	0.000	Autophagy
ATG4D	Autophagy	3.84	0.000	Autophagy
MLST8	Autophagy/mTor pathway	8.03	0.000	Autophagy
LAMTOR3	Modulates mTor pathway	5.37	0.000	NA
SIRT7	Neuroprotective during neurogenesis	4.64	0.004	NA
HTRA2	Aging/Cell and organ size/Neuroprotection	3.86	0.000	NA
CCDC22	NF-KB Regulation/Ritscher-Schinzel	6.95	0.000	NA
RGS14	Suppressed synaptic plasticity (LTP)	6.21	0.002	NA
DLGAP3	OCD	5.72	0.001	NA
EMC8	Protein homeostasis of GABAnergic neurons/ER membrane complex	3.42	0.021	NA
RGS4	GABAnergic/Photoperiod/Environmental processing	6.81	0.002	NA
RBFOX3	Promotes sleep/Associated with epilepsy	7.10	0.000	NA
B4GALNT1	Ganglioside synthesis/Promotes BACE1	4.30	0.008	NA

Literature cited

1. M. Arain, M. Haque, L. Johal, P. Mathur, W. Nel, A. Rais, R. Sandhu, S. Sharma, Maturation of the adolescent brain. *Neuropsychiatr. Dis. Treat.* **9**, 449–461 (2013).
2. S. J. Gould, Allometry and size in ontogeny and phylogeny. *Biol. Rev. Camb. Philos. Soc.* **41**, 587–640 (1966).
3. J. Lázaro, M. Hertel, M. Muturi, D. K. N. Dechmann, Seasonal reversible size changes in the braincase and mass of common shrews are flexibly modified by environmental conditions. *Sci. Rep.* **9**, 1–10 (2019).
4. Z. Pucek, Seasonal and age change in shrews as an adaptive process. *Symp. zool. Soc. Lond.* **26**, 189–207 (1970).
5. M. Pucek, Water contents and seasonal changes of the brain-weight in shrews. *Acta Theriol. (Warsz).* **10**, 353–367 (1965).
6. Z. Pucek, Seasonal and age changes in the weight of internal organs of shrews. *Acta Theriol. (Warsz).* **10**, 369–438 (1965).
7. L. Keicher, M. T. O'Mara, C. C. Voigt, D. K. N. Dechmann, Stable carbon isotopes in breath reveal fast metabolic incorporation rates and seasonally variable but rapid fat turnover in the common shrew (Sorex araneus). *J. Exp. Biol.* **220**, 2834–2841 (2017).
8. S. Churchfield, L. Rychlik, J. R. E. Taylor, Food resources and foraging habits of the common shrew, Sorex araneus: Does winter food shortage explain Dehnel's phenomenon? *Oikos*. **121**, 1593–1602 (2012).
9. J. R. E. Taylor, L. Rychlik, S. Churchfield, Winter reduction in body mass in a very small, nonhibernating mammal: Consequences for heat loss and metabolic rates. *Physiol. Biochem. Zool.* **86**, 9–18 (2013).
10. H. Hyvärinen, Wintering strategy of voles and shrews in Findland. *Winter Ecol. Small Mamm.* **10**, 139–148 (1984).
11. P. J. Schaeffer, M. T. O'Mara, J. Breiholz, L. Keicher, J. Lázaro, M. Muturi, D. K. N. Dechmann, Metabolic rate in common shrews is unaffected by temperature, leading to lower energetic costs through seasonal size reduction. *R. Soc. Open Sci.* **7** (2020), doi:10.1098/rsos.191989.
12. W. R. Thomas, D. K. N. Dechmann, J. Nieland, C. Baldoni, D. Carlson, D. Von Elverfeldt, J. Holm-jacobsen, M. Muturi, A. Corthals, M. Liliana, Molecular mechanisms of seasonal brain shrinkage and regrowth in Sorex araneus. *bioRxiv*, 1–16 (2023).
13. G. G. Auteri, L. L. Knowles, Decimated little brown bats show potential for adaptive change. *Sci. Rep.* **10**, 1–10 (2020).
14. F. Geiser, Ontogeny and phylogeny of endothermy and torpor in mammals and birds. *Comp. Biochem. Physiol. - A Mol. Integr. Physiol.* **150**, 176–180 (2008).
15. E. Ferris, C. Gregg, Parallel Accelerated Evolution in Distant Hibernators Reveals Candidate Cis Elements and Genetic Circuits Regulating Mammalian Obesity. *Cell Rep.* **29**, 2608–2620 (2019).
16. C. Turbill, C. Bieber, T. Ruf, Hibernation is associated with increased survival and the evolution of slow life histories among mammals. *Proc. R. Soc. B Biol. Sci.* **278**, 3355–3363 (2011).
17. S. L. Faherty, J. Luis Villanueva-Cañas, P. H. Klopfer, M. M. Albà, A. D. Yoder, Gene expression profiling in the hibernating primate, Cheirogaleus medius. *Genome Biol. Evol.* **8**, 2413–2426 (2016).
18. J. L. Villanueva-Cañas, S. L. Faherty, A. D. Yoder, M. M. Albà, Comparative genomics of mammalian hibernators using gene networks. *Integr. Comp. Biol.* **54**, 452–462 (2014).
19. M. Genoud, K. Isler, R. D. Martin, Comparative analyses of basal rate of metabolism in mammals□: data selection does matter. *Biol. Rev.* **93**, 404–438 (2018).
20. J. R. E. Taylor, "Evolution of Energetic Strategies in Shrews" in *Evolution of Shrews* (1998), pp. 309–346.
21. J. B. Searle, J. Zima, P. D. Polly, *Shrews, Chromosomes and Speciation* (Cambridge University Press, Cambridge, 2019).

22. K. Healy, T. Guillerme, S. Finlay, A. Kane, S. B. A. Kelly, D. McClean, D. J. Kelly, I. Donohue, A. L. Jackson, N. Cooper, Ecology and mode-of-life explain lifespan variation in birds and mammals. *Proc. R. Soc. B*. **281** (2014), doi:10.1098/rspb.2014.0298.
23. P. Mergenthaler, U. Lindauer, G. A. Dienel, A. Meisel, Sugar for the brain: The role of glucose in physiological and pathological brain function. *Trends Neurosci.* **36**, 587–597 (2013).
24. P. Nieminen, H. Hyvärinen, Seasonality of Leptin Levels in the BAT of the Common Shrew (Sorex araneus). *Z. Naturforsch.* **55**, 455–460 (2000).
25. N. Zeltser, I. Meyer, G. V. Hernandez, M. J. Trahan, R. K. Fanter, M. Abo-Ismail, H. Glanz, C. R. Strand, D. G. Burrin, M. R. la Frano, R. Manjarín, M. Maj, Neurodegeneration in juvenile Iberian pigs with diet-induced nonalcoholic fatty liver disease. *Am. J. Physiol. - Endocrinol. Metab.* **319**, E592–E606 (2020).
26. M. Vairetti, A. Ferrigno, V. Rizzo, G. Ambrosi, A. Bianchi, P. Richelmi, F. Blandini, M. T. Armentero, Impaired hepatic function and central dopaminergic denervation in a rodent model of Parkinson's disease: A self-perpetuating crosstalk? *Biochim. Biophys. Acta - Mol. Basis Dis.* **1822**, 176–184 (2012).
27. Z. Huang, H. W. Lin, Q. Zhang, X. Zong, Targeting Alzheimer's Disease: The Critical Crosstalk between the Liver and Brain. *Nutrients*. **14** (2022), doi:10.3390/nu14204298.
28. M. Trapecar, E. Wogram, D. Svoboda, C. Communal, A. Omer, T. Lungjangwa, P. Sphabmixay, J. Velazquez, K. Schneider, C. W. Wright, S. Mildrum, A. Hendricks, S. Levine, J. Muffat, M. J. Lee, D. A. Lauffenburger, D. Trumper, R. Jaenisch, L. G. Griffith, Human physiomimetic model integrating microphysiological systems of the gut, liver, and brain for studies of neurodegenerative diseases. *Sci. Adv.* **7** (2021), doi:10.1126/SCIADV.ABD1707.
29. S. Via, R. Lande, Genotype-environment interaction and the evolution of phenotypic plasticity. *Evolution (N. Y).* **39**, 505–522 (1985).
30. C. J. Brauer, P. J. Unmack, L. B. Beheregaray, Comparative ecological transcriptomics and the contribution of gene expression to the evolutionary potential of a threatened fish. *Mol. Ecol.* **26**, 6841–6856 (2017).
31. M. A. Bernal, C. Schunter, R. Lehmann, D. J. Lightfoot, B. J. M. Allan, H. D. Veilleux, J. L. Rummer, P. L. Munday, T. Ravasi, Species-specific molecular responses of wild coral reef fishes during a marine heatwave. *Sci. Adv.* **6**, 1–12 (2020).
32. D. B. Stern, K. A. Crandall, The evolution of gene expression underlying vision loss in cave animals. *Mol. Biol. Evol.* **35**, 2005–2014 (2018).
33. G. B. Gillard, L. Grønvold, L. L. Røsæg, M. M. Holen, Ø. Monsen, B. F. Koop, E. B. Rondeau, M. K. Gundappa, J. Mendoza, D. J. Macqueen, R. V. Rohlfs, S. R. Sandve, T. R. Hvidsten, Comparative regulomics supports pervasive selection on gene dosage following whole genome duplication. *Genome Biol.* **22**, 1–18 (2021).
34. G. C. Conant, The lasting after-effects of an ancient polyploidy on the genomes of teleosts. *PLoS One*. **15**, 1–26 (2020).
35. I. Braasch, A. R. Gehrke, J. J. Smith, K. Kawasaki, T. Manousaki, J. Pasquier, A. Amores, T. Desvignes, P. Batzel, J. Catchen, A. M. Berlin, M. S. Campbell, D. Barrell, K. J. Martin, J. F. Mulley, V. Ravi, A. P. Lee, T. Nakamura, D. Chalopin, S. Fan, D. Wcisel, C. Caestro, J. Sydes, F. E. G. Beaudry, Y. Sun, J. Hertel, M. J. Beam, M. Fasold, M. Ishiyama, J. Johnson, S. Kehr, M. Lara, J. H. Letaw, G. W. Litman, R. T. Litman, M. Mikami, T. Ota, N. R. Saha, L. Williams, P. F. Stadler, H. Wang, J. S. Taylor, Q. Fontenot, A. Ferrara, S. M. J. Searle, B. Aken, M. Yandell, I. Schneider, J. A. Yoder, J. N. Volff, A. Meyer, C. T. Amemiya, B. Venkatesh, P. W. H. Holland, Y. Guiguen, J. Bobe, N. H. Shubin, F. Di Palma, J. Alföldi, K. Lindblad-Toh, J. H. Postlethwait, The spotted gar genome illuminates vertebrate evolution and facilitates human-teleost comparisons. *Nat. Genet.* **48**, 427–437 (2016).
36. S. Lien, B. F. Koop, S. R. Sandve, J. R. Miller, M. P. Kent, T. Nome, T. R. Hvidsten, J. S. Leong, D. R. Minkley, A. Zimin, F. Grammes, H. Grove, A. Gjuvsland, B. Walenz, R. A. Hermansen, K. Von Schalburg, E. B. Rondeau, A. Di Genova, J. K. A. Samy, J. Olav Vik, M. D. Vigeland, L.

Caler, U. Grimholt, S. Jentoft, D. Inge Våge, P. De Jong, T. Moen, M. Baranski, Y. Palti, D. R. Smith, J. A. Yorke, A. J. Nederbragt, A. Tooming-Klunderud, K. S. Jakobsen, X. Jiang, D. Fan, Y. Hu, D. A. Liberles, R. Vidal, P. Iturra, S. J. M. Jones, I. Jonassen, A. Maass, S. W. Omholt, W. S. Davidson, The Atlantic salmon genome provides insights into rediploidization. *Nature*. **533**, 200–205 (2016).

37. S. R. Sandve, R. V. Rohlfs, T. R. Hvidsten, Subfunctionalization versus neofunctionalization after whole-genome duplication. *Nat. Genet.* **50**, 908–909 (2018).

38. T. F. Rogers, D. H. Palmer, A. E. Wright, Sex-Specific Selection Drives the Evolution of Alternative Splicing in Birds. *Mol. Biol. Evol.* **38**, 519–530 (2021).

39. R. V. Rohlfs, R. Nielsen, Phylogenetic ANOVA: The expression variance and evolution model for quantitative trait evolution. *Syst. Biol.* **64**, 695–708 (2015).

40. J. Chen, R. Swofford, J. Johnson, B. B. Cummings, N. Rogel, K. Lindblad-Toh, W. Haerty, F. di Palma, A. Regev, A quantitative model for characterizing the evolutionary history of mammalian gene expression. *bioRxiv*, 53–63 (2017).

41. E. Yapar, E. Saglican, H. M. Dönertaş, E. Özkurt, Z. Yan, H. Hu, S. Guo, B. Erdem, R. V. Rohlfs, P. Khaitovich, M. Somel, Convergent evolution of primate testis transcriptomes reflects mating strategy. *bioRxiv*, 1–25 (2021).

42. E. Sjöstedt, W. Zhong, L. Fagerberg, M. Karlsson, N. Mitsios, C. Adori, P. Oksvold, F. Edfors, A. Limiszewska, F. Hikmet, J. Huang, Y. Du, L. Lin, Z. Dong, L. Yang, X. Liu, H. Jiang, X. Xu, J. Wang, H. Yang, L. Bolund, A. Mardinoglu, C. Zhang, K. Von Feilitzen, C. Lindskog, F. Pontén, Y. Luo, T. Hökfelt, M. Uhlén, J. Mulder, An atlas of the protein-coding genes in the human, pig, and mouse brain. *Science (80-.).* **367**, 1–16 (2020).

43. J. Lázaro, M. Hertel, C. C. Sherwood, M. Muturi, D. K. N. Dechmann, Profound seasonal changes in brain size and architecture in the common shrew. *Brain Struct. Funct.* **223**, 2823–2840 (2018).

44. M. E. Pamenter, Adaptations to a hypoxic lifestyle in naked mole-rats. *J. Exp. Biol.* **225** (2022), doi:10.1242/jeb.196725.

45. M. O. Dietrich, T. L. Horvath, Hypothalamic control of energy balance: Insights into the role of synaptic plasticity. *Trends Neurosci.* **36**, 65–73 (2013).

46. S. Ramón y Cajal, Sur la fine structure du lobe optique des oiseaux et sur l'origine réelle des nerfs optiques. *J. Int. Anat. Physiol.* **7**, 1–30 (1891).

47. R. Apfelbach, D. Kruska, Postnatal development of the brain of the ferret Mustela putorius F Furo (Mustelidae, Mammalia). *Int. J. Mamm. Biol.* **44**, 127–131 (1979).

48. A. Singla, A. Fedoseienko, S. S. P. Giridharan, B. L. Overlee, A. Lopez, D. Jia, J. Song, K. Huff-Hardy, L. Weisman, E. Burstein, D. D. Billadeau, Endosomal PI(3)P regulation by the COMMD/CCDC22/CCDC93 (CCC) complex controls membrane protein recycling. *Nat. Commun.* **10** (2019), doi:10.1038/s41467-019-12221-6.

49. D. L. Tomasello, J. L. Kim, Y. Khodour, J. M. McCammon, M. Mitalipova, R. Jaenisch, A. H. Futerman, H. Sive, FAM57B is a modulator of ceramide synthesis that regulates sphingolipid homeostasis and synaptic composition in the developing brain. *bioRxiv*, 1–23 (2021).

50. A. Thathiah, K. Spittaels, M. Hoffmann, M. Staes, A. Cohen, K. Horré, M. Vanbrabant, F. Coun, V. Baekelandt, A. Delacourte, D. F. Fischer, D. Pollet, B. De Strooper, P. Merchiers, The orphan G protein-coupled receptor 3 modulates amyloid-beta peptide generation in neurons. *Science (80-.).* **323**, 946–951 (2009).

51. G. Godlewski, T. Jourdan, G. Szanda, J. Tam, R. Cinar, J. Harvey-White, J. Liu, B. Mukhopadhyay, P. Pacher, F. Ming Mo, D. Osei-Hyiaman, G. Kunos, Mice lacking GPR3 receptors display late-onset obese phenotype due to impaired thermogenic function in brown adipose tissue. *Sci. Rep.* **5**, 1–5 (2015).

52. E. J. Hoekstra, L. von Oerthel, L. P. van der Heide, W. M. Kouwenhoven, J. V. Veenvliet, I. Wever, Y. R. Jin, J. K. Yoon, A. J. A. van der Linden, F. C. P. Holstege, M. J. Groot Koerkamp, M. P. Smidt, Lmx1a Encodes a Rostral Set of Mesodiencephalic Dopaminergic Neurons Marked by the Wnt/B-Catenin Signaling Activator R-spondin 2. *PLoS One*. **8**, 1–12 (2013).

53. L. Pedersen, P. Panahandeh, M. I. Siraji, S. Knappskog, P. E. Lønning, R. Gordillo, P. E. Scherer, A. Molven, K. Teigen, N. Halberg, Golgi-localized PAQR4 mediates antiapoptotic ceramidase activity in breast cancer. *Cancer Res.* **80**, 2163–2174 (2020).
54. B. M. C. McGowan, S. A. Stanley, M. A. Ghatei, S. R. Bloom, "Relaxin-3 and its role in neuroendocrine function" in *Annals of the New York Academy of Sciences* (2009), vol. 1160, pp. 250–255.
55. C. M. Smith, P. J. Ryan, I. T. Hosken, S. Ma, A. L. Gundlach, Relaxin-3 systems in the brain — The first 10 years. *J. Chem. Neuroanat. jo.* **42**, 262–275 (2011).
56. H. Otsubo, T. Onaka, H. Suzuki, A. Katoh, T. Ohbuchi, M. Todoroki, M. Kobayashi, H. Fujihara, T. Yokoyama, T. Matsumoto, Y. Ueta, Centrally administered relaxin-3 induces Fos expression in the osmosensitive areas in rat brain and facilitates water intake. *Peptides*. **31**, 1124–1130 (2010).
57. B. M. C. McGowan, S. A. Stanley, K. L. Smith, N. E. White, M. M. Connolly, E. L. Thompson, J. V. Gardiner, K. G. Murphy, M. A. Ghatei, S. R. Bloom, Central relaxin-3 administration causes hyperphagia in male wistar rats. *Endocrinology*. **146**, 3295–3300 (2005).
58. C. Lenglos, A. Mitra, G. Guèvremont, E. Timofeeva, Sex differences in the effects of chronic stress and food restriction on body weight gain and brain expression of CRF and relaxin-3 in rats. *Genes, Brain Behav.* **12**, 370–387 (2013).
59. C. De Ávila, S. Chometton, C. Lenglos, J. Calvez, A. L. Gundlach, E. Timofeeva, Differential effects of relaxin-3 and a selective relaxin-3 receptor agonist on food and water intake and hypothalamic neuronal activity in rats. *Behav. Brain Res.* **336**, 135–144 (2018).
60. J. Calvez, C. Lenglos, C. de Ávila, G. Guèvremont, E. Timofeeva, Differential effects of central administration of relaxin-3 on food intake and hypothalamic neuropeptides in male and female rats. *Genes, Brain Behav.* **14**, 550–563 (2015).
61. C. Lenglos, J. Calvez, E. Timofeeva, Sex-specific effects of relaxin-3 on food intake and brain expression of corticotropin-releasing factor in rats. *Endocrinology*. **156**, 523–533 (2015).
62. B. M. C. McGowan, S. A. Stanley, N. E. White, A. Spangeus, M. Patterson, E. L. Thompson, K. L. Smith, J. Donovan, J. V. Gardiner, M. A. Ghatei, S. R. Bloom, Hypothalamic mapping of orexigenic action and Fos-like immunoreactivity following relaxin-3 administration in male Wistar rats. *Am. J. Physiol. - Endocrinol. Metab.* **292**, 913–919 (2007).
63. N. Ahmad, W. Wang, R. Nair, S. Kapila, Relaxin induces matrix-metalloproteinases-9 and -13 via RXFP1: Induction of MMP-9 involves the PI3K, ERK, Akt and PKC-ζ pathways. *Mol. Cell. Endocrinol.* **363**, 46–61 (2012).
64. C. W. Dessauer, B. T. Nguyen, Relaxin stimulates multiple signaling pathways: Activation of cAMP, PI3K, and PKCζ in THP-1 cells. *Ann. N. Y. Acad. Sci.* **1041**, 272–279 (2005).
65. L. Shen, D. Q. Wang, P. Tso, R. J. Jandacek, S. C. Woods, M. Liu, Physiology & Behavior Apolipoprotein E reduces food intake via PI3K / Akt signaling pathway in the hypothalamus. *Physiol. Behav.* **105**, 124–128 (2011).
66. L. Shen, C. C. Lo, L. A. Woollett, M. Liu, Biochemical and Biophysical Research Communications Apolipoprotein A-IV exerts its anorectic action through a PI3K / Akt signaling pathway in the hypothalamus. *Biochem. Biophys. Res. Commun.* **494**, 152–157 (2017).
67. K. D. Niswender, G. J. Morton, W. H. Stearns, C. J. Rhodes, M. G. Myers, M. W. Schwartz, Intracellular signalling: Key enzyme in leptin-induced anorexia. *Nature*. **413**, 794–795 (2001).
68. A. C. Könner, R. Janoschek, L. Plum, S. D. Jordan, E. Rother, X. Ma, C. Xu, P. Enriori, B. Hampel, G. S. Barsh, C. R. Kahn, M. A. Cowley, F. M. Ashcroft, J. C. Brüning, Insulin Action in AgRP-Expressing Neurons Is Required for Suppression of Hepatic Glucose Production. *Cell Metab.* **5**, 438–449 (2007).
69. J. W. Hill, Y. Xu, F. Preitner, M. Fukuda, Y. R. Cho, J. Luo, N. Balthasar, R. Coppari, L. C. Cantley, B. B. Kahn, J. J. Zhao, J. K. Elmquist, Phosphatidyl inositol 3-kinase signaling in hypothalamic proopiomelanocortin neurons contributes to the regulation of glucose homeostasis. *Endocrinology*. **150**, 4874–4882 (2009).
70. J. Karar, A. Maity, PI3K/AKT/mTOR Pathway in Angiogenesis. *Front. Mol. Neurosci.* **4**, 1–8

(2011).
71. A. Maity, N. Pore, J. Lee, D. Solomon, D. onald M. O'Rourke, Epidermal growth factor receptor transcriptionally up-regulates vascular endothelial growth factor expression in human glioblastoma cells via a pathway involving phosphatidylinositol 3'-kinase and distinct from that induced by hypoxia. *Cancer Res.* **60**, 5879–5886 (2000).
72. C. M. Taniguchi, B. Emanuelli, C. R. Kahn, Critical nodes in signalling pathways: insights into insulin action. *Nat. Rev. Mol. Cell Biol.* **7**, 85–96 (2006).
73. Z. Li, X. Liu, P. Zhang, R. Han, G. Sun, R. Jiang, Y. Wang, X. Liu, Comparative transcriptome analysis of hypothalamus-regulated feed intake induced by exogenous visfatin in chicks. *BMC Genomics*. **19**, 1–17 (2018).
74. B. Chen, W. Fang, Y. Li, T. Xiong, M. Zhou, L. Wan, Q. Liu, W. Zhang, X. Hu, H. Mao, S. Liu, RNA-seq and differential expression analysis of the duck transcriptome□: The effect of short-term cage-rearing. *bioRxiv* (2021), doi:https://doi.org/10.1101/2021.05.13.444049.
75. J.-M. Kim, K.-S. Lim, M. Byun, K.-T. Lee, Y.-R. Yang, M. Park, D. Lim, H.-H. Chai, H.-T. Bang, J. Hwangbo, Y.-H. Choi, Y.-M. Cho, J.-E. Park, Identification of the acclimation genes in transcriptomic responses to heat stress of White Pekin duck. *Cell Stress Chaperones*. **22**, 787–797 (2017).
76. X. Y. Chen, R. Li, M. Wang, Z. Y. Geng, Identification of differentially expressed genes in hypothalamus of chicken during cold stress. *Miol Biol Rep*. **41**, 2243–2248 (2014).
77. W. Ma, G. Fuentes, X. Shi, C. Verma, G. K. Radda, W. Han, FoxO1 negatively regulates leptin-induced POMC transcription through its direct interaction with STAT3. *Biochem. J.* **466**, 291–298 (2015).
78. M. Amitani, A. Asakawa, H. Amitani, A. Inui, The role of leptin in the control of insulin-glucose axis. *Front. Neurosci.* **7**, 1–12 (2013).
79. T. Sasaki, H. J. Kim, M. Kobayashi, Y. I. Kitamura, H. Yokota-Hashimoto, T. Shiuchi, Y. Minokoshi, T. Kitamura, Induction of hypothalamic Sirt1 leads to cessation of feeding via agouti-related peptide. *Endocrinology*. **151**, 2556–2566 (2010).
80. J. Nakae, Y. Cao, H. Daitoku, A. Fukamizu, W. Ogawa, Y. Yano, Y. Hayashi, The LXXLL motif of murine forkhead transcription factor FoxO1 mediates Sirt1-dependent transcriptional activity. *J. Clin. Invest.* **116**, 2473–2483 (2006).
81. B. Wang, J. Zhu, K. Mounzih, E. F. Chehab, Y. Ke, F. F. Chehab, Overexpression of the transcription factor foxo4 is associated with rapid glucose clearance. *Mol. Cell. Endocrinol.* **307**, 217–223 (2009).
82. A. Tups, S. Stöhr, M. Helwig, P. Barrett, E. Krol, J. Schachtner, J. G. Mercer, M. Klingenspor, Seasonal leptin resistance is associated with impaired signalling via JAK2-STAT3 but not ERK, possibly mediated by reduced hypothalamic GRB2 protein. *J. Comp. Physiol. B Biochem. Syst. Environ. Physiol.* **182**, 553–567 (2012).
83. J. E. Son, Z. Dou, K. H. Kim, C. C. Hui, Deficiency of Irx5 protects mice from obesity and associated metabolic abnormalities. *Int. J. Obes.* **46**, 2029–2039 (2022).
84. J. E. Son, Z. Dou, K. H. Kim, S. Wanggou, V. S. Bin Cha, R. Mo, X. Zhang, X. Chen, T. Ketela, X. Li, X. Huang, C. chung Hui, Irx3 and Irx5 in Ins2-Cre + cells regulate hypothalamic postnatal neurogenesis and leptin response. *Nat. Metab.* **3**, 701–713 (2021).
85. S. Raab, H. Beck, A. Gaumann, A. Yüce, H. P. Gerber, K. Plate, H. P. Hammes, N. Ferrara, G. Breier, Impaired brain angiogenesis and neuronal apoptosis induced by conditional homozygous inactivation of vascular endothelial growth factor. *Thromb. Haemost.* **91**, 595–605 (2004).
86. P. Carmeliet, V. Ferreira, G. Breier, S. Pollefeyt, L. Kieckens, M. Gertsenstein, M. Fahrig, A. Vandenhoeck, K. Harpal, C. Eberhardt, C. Declercq, J. Pawling, L. Moons, D. Collen, W. Risau, A. Nagy, Abnormal blood vessel development and lethality in embryos lacking a single vascular endothelial growth factor allele. *Nature*. **380**, 435–439 (1996).
87. R. Daneman, D. Agalliu, L. Zhou, F. Kuhnert, C. J. Kuo, B. A. Barres, Wnt/β-catenin signaling is required for CNS, but not non-CNS, angiogenesis. *Proc. Natl. Acad. Sci. U. S. A.* **106**, 641–646

(2009).
88. A. T. Argaw, L. Asp, J. Zhang, K. Navrazhina, T. Pham, J. N. Mariani, S. Mahase, D. J. Dutta, J. Seto, E. G. Kramer, N. Ferrara, M. V. Sofroniew, G. R. John, Astrocyte-derived VEGF-A drives blood-brain barrier disruption in CNS inflammatory disease. *J. Clin. Invest.* **122**, 2454–2468 (2012).
89. H. Kim, J. M. Lee, J. S. Park, S. A. Jo, Y. O. Kim, C. W. Kim, I. Jo, Dexamethasone coordinately regulates angiopoietin-1 and VEGF: A mechanism of glucocorticoid-induced stabilization of blood-brain barrier. *Biochem. Biophys. Res. Commun.* **372**, 243–248 (2008).
90. A. T. Argaw, B. T. Gurfein, Y. Zhang, A. Zameer, G. R. John, VEGF-mediated disruption of endothelial CLN-5 promotes blood-brain barrier breakdown. *Proc. Natl. Acad. Sci. U. S. A.* **106**, 1977–1982 (2009).
91. G. Lan, P. Wang, R. B. Chan, Z. Liu, Z. Yu, X. Liu, Y. Yang, J. Zhang, Astrocytic VEGFA: An essential mediator in blood–brain-barrier disruption in Parkinson's disease. *Glia*. **70**, 337–353 (2022).
92. B. Obermeier, R. Daneman, R. M. Ransohoff, Development, maintenance and disruption of the blood-brain barrier. *Nat. Med.* **19**, 1584–1596 (2013).
93. L. Bennett, M. Yang, G. Enikolopov, L. Iacovitti, Circumventricular organs: A novel site of neural stem cells in the adult brain. *Mol. Cell. Neurosci.* **41**, 337–347 (2009).
94. F. Langlet, B. E. Levin, S. Luquet, M. Mazzone, A. Messina, A. A. Dunn-Meynell, E. Balland, A. Lacombe, D. Mazur, P. Carmeliet, S. G. Bouret, V. Prevot, B. Dehouck, Tanycytic VEGF-A boosts blood-hypothalamus barrier plasticity and access of metabolic signals to the arcuate nucleus in response to fasting. *Cell Metab.* **17**, 607–617 (2013).
95. R. Haddad-Tóvolli, N. R. V. Dragano, A. F. S. Ramalho, L. A. Velloso, Development and function of the blood-brain barrier in the context of metabolic control. *Front. Neurosci.* **11**, 1–12 (2017).
96. T. K. T. Lam, G. J. Schwartz, L. Rossetti, Hypothalamic sensing of fatty acids. *Nat. Neurosci.* **8**, 579–584 (2005).
97. P.-M. Chevillard, M. Batailler, B. Piégu, A. Estienne, M.-C. Blache, J.-P. Dubois, D. Pillon, P. Vaudin, J. Dupont, N. Just, M. Migaud, Seasonal vascular plasticity in the mediobasal hypothalamus of the adult ewe. *Histochem. Cell Biol.* **157**, 581–593 (2022).
98. J. Castle-Miller, D. O. Bates, D. J. Tortonese, Mechanisms regulating angiogenesis underlie seasonal control of pituitary function. *Proc. Natl. Acad. Sci. U. S. A.* **114**, E2514–E2523 (2017).
99. A. Tabecka-Lonczynska, J. Mytych, P. Solek, A. Abrachamowicz, M. Welz, M. Koziorowski, Local regulators of seasonal reproduction processes in uterus masculinus of an adult male european bison (bison bonasus, linnaeus 1758). *J. Physiol. Pharmacol.* **69**, 747–753 (2018).
100. Y. Yao, W. Xie, D. Chen, Y. Han, Z. Yuan, H. Zhang, Q. Weng, Seasonal expressions of VEGF and its receptors VEGFR1 and VEGFR2 in the prostate of the wild ground squirrels (Spermophilus dauricus). *Eur. J. Histochem.* **65**, 35219 (2021).
101. M. B. Ahrens, M. B. Orger, D. N. Robson, J. M. Li, P. J. Keller, Whole-brain functional imaging at cellular resolution using light-sheet microscopy. *Nat. Methods*. **10**, 413–420 (2013).
102. K. Mann, C. L. Gallen, T. R. Clandinin, Whole-Brain Calcium Imaging Reveals an Intrinsic Functional Network in Drosophila. *Curr. Biol.* **27**, 2389–2396 (2017).
103. S. B. Kater, M. P. Mattson, C. Cohan, J. Connor, Calcium regulation of the neuronal growth cone. *Trends Neurosci.* **11**, 315–321 (1988).
104. M. P. Mattson, Neurotransmitters in the regulation of neuronal cytoarchitecture. *Brain Res. Rev.* **472**, 179–212 (1988).
105. K. Deisseroth, H. Bito, R. W. Tsien, Signaling from synapse to nucleus: Postsynaptic CREB phosphorylation during multiple forms of hippocampal synaptic plasticity. *Neuron*. **16**, 89–101 (1996).
106. H. Bito, K. Deisseroth, R. W. Tsien, Ca2+-dependent regulation in neuronal gene expression. *Curr. Opin. Neurobiol.* **7**, 419–429 (1997).

107. M. J. Berridge, Neuronal calcium. *Neuron*. **21**, 13–26 (1998).
108. S. J. Zhang, M. Zou, L. Lu, D. Lau, D. A. W. Ditzel, C. Delucinge-Vivier, Y. Aso, P. Descombes, H. Bading, Nuclear calcium signaling controls expression of a large gene pool: Identification of a gene program for acquired neuroprotection induced by synaptic activity. *PLoS Genet.* **5** (2009), doi:10.1371/journal.pgen.1000604.
109. L. Redmond, A. Ghosh, Regulation of dendritic development by calcium signaling. *Cell Calcium*. **37**, 411–416 (2005).
110. C. Lohmann, R. O. L. Wong, Regulation of dendritic growth and plasticity by local and global calcium dynamics. *Cell Calcium*. **37**, 403–409 (2005).
111. H. Kazama, A. Nose, T. Morimoto-Tanifuji, Synaptic components necessary for retrograde signaling triggered by calcium/calmodulin-dependent protein kinase II during synaptogenesis. *Neuroscience*. **145**, 1007–1015 (2007).
112. C. Verderio, S. Coco, G. Fumagalli, M. Matteoli, Spatial changes in calcium signaling during the establishment of neuronal polarity and synaptogenesis. *J. Cell Biol.* **126**, 1527–1536 (1994).
113. K. Michaelsen, C. Lohmann, Calcium dynamics at developing synapses: Mechanisms and functions. *Eur. J. Neurosci.* **32**, 218–223 (2010).
114. R. C. Malenka, J. A. Kauer, R. S. Zucker, R. A. Nicoll, Postsynaptic Calcium Is Sufficient for Potentiation of Hippocampal Synaptic Transmission. *Science (80-.).* **242**, 81–84 (1988).
115. S. Poser, D. R. Storm, Role of Ca2+-stimulated adenylyl cyclases in LTP and memory formation. *Int. J. Dev. Neurosci.* **19**, 387–394 (2001).
116. H. Bading, Nuclear calcium signalling in the regulation of brain function. *Nat. Rev. Neurosci.* **14**, 593–608 (2013).
117. H. Bading, Transcription-dependent neuronal plasticity. *Eur. J. Biochem.* **267**, 5280–5283 (2000).
118. G. J. Augustine, F. Santamaria, K. Tanaka, Local Calcium Signaling in Neurons. *Neuron*. **40**, 331–346 (2003).
119. S. Finkbeiner, M. E. Greenberg, Spatial features of calcium-regulated gene expression. *BioEssays*. **19**, 657–660 (1997).
120. H. L. Haas, U. M. Bucher, Histamine H2-receptors on single central neurones. *Nature*. **255**, 634–635 (1975).
121. H. elmu. L. Haas, A. Konnerth, Histamine and noradrenaline decrease calcium-activated potassium conductance in hippocampal pyramidal cells. *Nature*. **302**, 432–434 (1983).
122. H. L. Haas, O. A. Sergeeva, O. Selbach, Histamine in the nervous system. *Physiol. Rev.* **88**, 1183–1241 (2008).
123. S. Yuh Liou, S. Shibata, K. Yamakawa, S. Ueki, Inhibitory and excitatory effects of histamine on suprachiasmatic neurons in rat hypothalamic slice preparation. *Neurosci. Lett.* **41**, 109–113 (1983).
124. A. Lecklin, P. Etu-Seppälä, H. Stark, L. Tuomisto, Effects of intracerebroventricularly infused histamine and selective H1, H2 and H3 agonists on food and water intake and urine flow in Wistar rats. *Brain Res.* **793**, 279–288 (1998).
125. T. Masaki, S. Chiba, T. Yasuda, H. Noguchi, T. Kakuma, T. Watanabe, T. Sakata, H. Yoshimatsu, Involvement of hypothalamic histamine H1 receptor in the regulation of feeding rhythm and obesity. *Diabetes*. **53**, 2250–2260 (2004).
126. E. H. Schneider, D. Neumann, R. Seifert, Modulation of behavior by the histaminergic system: Lessons from H1R-and H2R-deficient mice. *Neurosci. Biobehav. Rev.* **42**, 252–266 (2014).
127. D. A. Guertin, D. M. Stevens, C. C. Thoreen, A. A. Burds, N. Y. Kalaany, J. Moffat, M. Brown, K. J. Fitzgerald, D. M. Sabatini, Ablation in Mice of the mTORC Components raptor, rictor, or mLST8 Reveals that mTORC2 Is Required for Signaling to Akt-FOXO and PKCα, but Not S6K1. *Dev. Cell*. **11**, 859–871 (2006).
128. R. A. Saxton, D. M. Sabatini, mTOR Signaling in Growth, Metabolism, and Disease. *Cell*. **168**, 960–976 (2017).
129. C. P. Baines, R. A. Kaiser, N. H. Purcell, N. S. Blair, H. Osinska, M. A. Hambleton, E. W. Brunskill, M. R. Sayen, R. A. Gottlieb, G. W. Dorn, J. Robbins, J. D. Molkentin, Loss of

cyclophilin D reveals a critical role for mitochondrial permeability transition in cell death. *Nature*. **434**, 984–984 (2004).

130. Takashi Nakagawa, Shigeomi Shimizu, Tetsuya Watanabe, Osamu Yamaguchi, Kinya Otsu, Hirotaka Yamagata, Hidenori Inohara, Takeshi Kubo, Yoshihide Tsujimoto, Cyclophilin D-dependentmitochondrial permeabilitytransition regulates some necroticbut not apoptotic cell death. *Nature*. **434**, 648–652 (2005).

131. V. Li, T. Brustovetsky, N. Brustovetsky, Role of cyclophilin D-dependent mitochondrial permeability transition in glutamate-induced calcium deregulation and excitotoxic neuronal death. *Exp. Neurol.* **218**, 171–182 (2009).

132. A. P. Halestrap, A pore way to die. *Nature*. **430**, 984–984 (2004).

133. M. Maceyka, H. Sankala, N. C. Hait, H. Le Stunff, H. Liu, R. Toman, C. Collier, M. Zhang, L. S. Satin, A. H. Merrill, S. Milstien, S. Spiegel, SphK1 and SphK2, sphingosine kinase isoenzymes with opposing functions in sphingolipid metabolism. *J. Biol. Chem.* **280**, 37118–37129 (2005).

134. H. Liu, R. E. Toman, S. K. Goparaju, M. Maceyka, V. E. Nava, H. Sankala, S. G. Payner, M. Bektas, I. Ishii, J. Chun, S. Milstien, S. Spiegel, Sphingosine kinase type 2 is a putative BH3-only protein that induces apoptosis. *J. Biol. Chem.* **278**, 40330–40336 (2003).

135. J. F. Moruno-Manchon, N. E. Uzor, M. P. Blasco-Conesa, S. Mannuru, N. Putluri, E. E. Furr-Stimming, A. S. Tsvetkov, Inhibiting sphingosine kinase 2 mitigates mutant Huntingtin-induced neurodegeneration in neuron models of Huntington disease. *Hum. Mol. Genet.* **26**, 1305–1317 (2017).

136. N. Takasugi, T. Sasaki, K. Suzuki, S. Osawa, H. Isshiki, Y. Hori, N. Shimada, T. Higo, S. Yokoshima, T. Fukuyama, V. M. Y. Lee, J. Q. Trojanowski, T. Tomita, T. Iwatsubo, BACE1 activity is modulated by cell-associated sphingosine-1-phosphate. *J. Neurosci.* **31**, 6850–6857 (2011).

137. H. Du, L. Guo, F. Fang, D. Chen, A. A Sosunov, G. M McKhann, Y. Yan, C. Wang, H. Zhang, J. D. Molkentin, F. J. Gunn-Moore, J. P. Vonsattel, O. Arancio, J. X. Chen, S. Du Yan, Cyclophilin D deficiency attenuates mitochondrial and neuronal perturbation and ameliorates learning and memory in Alzheimer's disease. *Nat. Med.* **14**, 1097–1105 (2008).

138. H. Du, L. Guo, W. Zhang, M. Rydzewska, S. Yan, Cyclophilin D deficiency improves mitochondrial function and learning/memory in aging Alzheimer disease mouse model. *Neurobiol. Aging*. **32**, 398–406 (2011).

139. B. Smith, thesis, Max Planck Institute for Ornithology (2016).

140. C. C. Fleck, H. V. Carey, Modulation of apoptotic pathways in intestinal mucosa during hibernation. *Am. J. Physiol. - Regul. Integr. Comp. Physiol.* **289**, 586–595 (2005).

141. S. M. Logan, S. N. Tessier, J. Tye, K. B. Storey, Response of the JAK-STAT pathway to mammalian hibernation in 13-lined ground squirrel striated muscle. *Mol. Cell. Biochem.* **414**, 115–127 (2016).

142. A. N. Rouble, J. Hefler, H. Mamady, K. B. Storey, S. N. Tessier, Anti-apoptotic signaling as a cytoprotective mechanism in mammalian hibernation. *PeerJ*. **2013**, 1–21 (2013).

143. A. Vicario, L. Kisiswa, J. Y. Tann, C. E. Kelly, C. F. Ibáñez, Neuron-type-specific signaling by the p75NTR death receptor is regulated by differential proteolytic cleavage. *J. Cell Sci.* **128**, 1507–1517 (2015).

144. G. Khursigara, J. Bertin, H. Yano, H. Moffett, P. S. DiStefano, M. V. Chao, A prosurvival function for the p75 receptor death domain mediated via the caspase recruitment domain receptor-interacting protein 2. *J. Neurosci.* **21**, 5854–5863 (2001).

145. B. D. Carter, C. Kaltschmidt, B. Kaltschmidt, R. Böhm-matthaei, P. A. Baeuerle, Y. Barde, Selective Activation of NF-κB by Nerve Growth Factor Through the Neurotrophin Receptor p75. *Science (80-.)*. **272**, 542–545 (1996).

146. A. L. Bhakar, L. L. Tannis, C. Zeindler, M. P. Russo, C. Jobin, D. S. Park, S. MacPherson, P. A. Barker, Constitutive nuclear factor-κB activity is required for central neuron survival. *J. Neurosci.* **22**, 8466–8475 (2002).

147. N. T. Bui, A. Livolsi, J. F. Peyron, J. H. M. Prehn, Activation of nuclear factor κB and bcl-x survival gene expression by nerve growth factor requires tyrosine phosphorylation of IκBα. *J. Cell Biol.* **152**, 753–763 (2001).
148. N. Motoyama, F. Wang, K. A. Roth, H. Sawa, K. Nakayama, I. Negishi, S. Senju, Q. Zhang, S. Fujii, D. Y. Loh, N. Motoyama, F. Wang, K. A. Roth, H. Sawa, K. Nakayama, K. Nakayama, I. Negishi, S. Senju, Q. Zhang, S. Fujii, D. Y. Loht, Massive Cell Death of Immature Hematopoietic Cells and Neurons in Bcl-x-Deficient Mice. *Science (80-.).* **267**, 1506–1510 (1995).
149. L. H. Boise, C. B. Thompson, Bcl-XL can inhibit apoptosis in cells that have undergone Fas-induced protease activation. *Proc. Natl. Acad. Sci. U. S. A.* **94**, 3759–3764 (1997).
150. C. A. Phillips-Krawczak, A. Singla, P. Starokadomskyy, Z. Deng, D. G. Osborne, H. Li, C. J. Dick, T. S. Gomez, M. Koenecke, J. S. Zhang, H. Dai, L. F. Sifuentes-Dominguez, L. N. Geng, S. H. Kaufmann, M. Y. Hein, M. Wallis, J. McGaughran, J. Gecz, B. Van De Sluis, D. D. Billadeau, E. Burstein, COMMD1 is linked to the WASH complex and regulates endosomal trafficking of the copper transporter ATP7A. *Mol. Biol. Cell*. **26**, 91–103 (2015).
151. P. Bartuzi, D. D. Billadeau, R. Favier, S. Rong, D. Dekker, A. Fedoseienko, H. Fieten, M. Wijers, J. H. Levels, N. Huijkman, N. Kloosterhuis, H. Van Der Molen, G. Brufau, A. K. Groen, A. M. Elliott, J. A. Kuivenhoven, B. Plecko, G. Grangl, J. McGaughran, J. D. Horton, E. Burstein, M. H. Hofker, B. Van De Sluis, CCC- and WASH-mediated endosomal sorting of LDLR is required for normal clearance of circulating LDL. *Nat. Commun.* **7**, 1–11 (2016).
152. D. C. Rubinsztein, The roles of intracellular protein-degradation pathways in neurodegeneration. *Nature*. **443**, 780–786 (2006).
153. F. J. McDonald, Explosion in the complexity of membrane protein recycling. *Am. J. Physiol. - Cell Physiol.* **320**, C483–C494 (2021).
154. L. Muzio, R. Sirtori, D. Gornati, S. Eleuteri, A. Fossaghi, D. Brancaccio, L. Manzoni, L. Ottoboni, L. De Feo, A. Quattrini, E. Mastrangelo, L. Sorrentino, E. Scalone, G. Comi, L. Marinelli, N. Riva, M. Milani, P. Seneci, G. Martino, Retromer stabilization results in neuroprotection in a model of Amyotrophic Lateral Sclerosis. *Nat. Commun.* **11**, 1–17 (2020).
155. S. A. Small, K. Kent, A. Pierce, C. Leung, M. S. Kang, H. Okada, L. Honig, J. P. Vonsattel, T. W. Kim, Model-guided microarray implicates the retromer complex in Alzheimer's disease. *Ann. Neurol.* **58**, 909–919 (2005).
156. E. Rogaeva, Y. Meng, J. H. Lee, Y. Gu, T. Kawarai, F. Zou, T. Katayama, C. T. Baldwin, R. Cheng, H. Hasegawa, F. Chen, N. Shibata, K. L. Lunetta, R. Pardossi-Piquard, C. Bohm, Y. Wakutani, L. A. Cupples, K. T. Cuenco, R. C. Green, L. Pinessi, I. Rainero, S. Sorbi, A. Bruni, R. Duara, R. P. Friedland, R. Inzelberg, W. Hampe, H. Bujo, Y. Q. Song, O. M. Andersen, T. E. Willnow, N. Graff-Radford, R. C. Petersen, D. Dickson, S. D. Der, P. E. Fraser, G. Schmitt-Ulms, S. Younkin, R. Mayeux, L. A. Farrer, P. St. George-Hyslop, The neuronal sortilin-related receptor SORL1 is genetically associated with Alzheimer disease. *Nat. Genet.* **39**, 168–177 (2007).
157. R. F. Lane, S. M. Raines, J. W. Steele, M. E. Ehrlich, J. A. Lah, S. A. Small, R. E. Tanzi, A. D. Attie, S. Gandy, Diabetes-associated SorCS1 regulates Alzheimer's amyloid-β metabolism: Evidence for involvement of SorL1 and the retromer complex. *J. Neurosci.* **30**, 13110–13115 (2010).
158. F. L. Tang, W. Liu, J. X. Hu, J. R. Erion, J. Ye, L. Mei, W. C. Xiong, VPS35 Deficiency or Mutation Causes Dopaminergic Neuronal Loss by Impairing Mitochondrial Fusion and Function. *Cell Rep.* **12**, 1631–1643 (2015).
159. I. Voineagu, L. Huang, K. Winden, M. Lazaro, E. Haan, J. Nelson, J. McGaughran, L. S. Nguyen, K. Friend, A. Hackett, M. Field, J. Gecz, D. Geschwind, CCDC22: A novel candidate gene for syndromic X-linked intellectual disability. *Mol. Psychiatry*. **17**, 4–7 (2012).
160. M. Kolanczyk, P. Krawitz, J. Hecht, A. Hupalowska, M. Miaczynska, K. Marschner, C. Schlack, D. Emmerich, K. Kobus, U. Kornak, P. N. Robinson, B. Plecko, G. Grangl, S. Uhrig, S. Mundlos, D. Horn, Missense variant in CCDC22 causes X-linked recessive intellectual disability with features of Ritscher-Schinzel/3C syndrome. *Eur. J. Hum. Genet.* **23**, 633–638 (2015).

161. S. Neri, N. Maia, A. M. Fortuna, J. Damasio, E. Coale, M. Willis, P. Jorge, A. F. Højte, C. D. Fenger, R. S. Møller, A. Bayat, Expanding the pre- and postnatal phenotype of WASHC5 and CCDC22 -related Ritscher-Schinzel syndromes. *Eur. J. Med. Genet.* **65**, 1–7 (2022).
162. C. E. Gjerulfsen, R. S. Møller, C. D. Fenger, T. B. Hammer, A. Bayat, Expansion of the CCDC22 associated ritscher-schinzel/3C syndrome and review of the literature: Should the minimal diagnostic criteria be revised? *Eur. J. Med. Genet.* **64** (2021), doi:10.1016/j.ejmg.2021.104246.
163. T. Portmann, M. Yang, R. Mao, G. Panagiotakos, J. Ellegood, G. Dolen, P. L. Bader, B. A. Grueter, C. Goold, E. Fisher, K. Clifford, P. Rengarajan, D. Kalikhman, D. Loureiro, N. L. Saw, Z. Zhengqui, M. A. Miller, J. P. Lerch, R. M. Henkelman, M. Shamloo, R. C. Malenka, J. N. Crawley, R. E. Dolmetsch, Behavioral abnormalities and circuit defects in the basal ganglia of a mouse model of 16p11.2 deletion syndrome. *Cell Rep.* **7**, 1077–1092 (2014).
164. J. M. McCammon, A. Blaker-Lee, X. Chen, H. Sive, The 16p11.2 homologs fam57ba and doc2a generate certain brain and body phenotypes. *Hum. Mol. Genet.* **26**, 3699–3712 (2017).
165. L. A. Weiss, Y. Shen, J. M. Korn, D. E. Arking, D. T. Miller, R. Fossdal, E. Saemundsen, H. Stefansson, M. A. R. Ferreira, T. Green, O. S. Platt, D. M. Ruderfer, C. A. Walsh, D. Altshuler, A. Chakravarti, R. E. Tanzi, K. Stefansson, S. L. Santangelo, J. F. Gusella, P. Sklar, B.-L. Wu, M. J. Daly, Association between Microdeletion and Microduplication at 16p11.2 and Autism. *N. Engl. J. Med.* **358**, 667–675 (2008).
166. T. Arbogast, A. M. Ouagazzal, C. Chevalier, M. Kopanitsa, N. Afinowi, E. Migliavacca, B. S. Cowling, M. C. Birling, M. F. Champy, A. Reymond, Y. Herault, Reciprocal Effects on Neurocognitive and Metabolic Phenotypes in Mouse Models of 16p11.2 Deletion and Duplication Syndromes. *PLoS Genet.* **12**, 1–35 (2016).
167. Y. Qiu, T. Arbogast, S. M. Lorenzo, H. Li, S. C. Tang, E. Richardson, O. Hong, S. Cho, O. Shanta, T. Pang, C. Corsello, C. K. Deutsch, C. Chevalier, E. E. Davis, L. M. Iakoucheva, Y. Herault, N. Katsanis, K. Messer, J. Sebat, Oligogenic Effects of 16p11.2 Copy-Number Variation on Craniofacial Development. *Cell Rep.* **28**, 3320-3328.e4 (2019).
168. A. Blaker-Lee, S. Gupta, J. M. McCammon, G. De Rienzo, H. Sive, Zebrafish homologs of genes within 16p11.2, a genomic region associated with brain disorders, are active during brain development, and include two deletion dosage sensor genes. *Dis. Model. Mech.* **5**, 834–851 (2012).
169. Y. Yamashita-Sugahara, Y. Tokuzawa, Y. Nakachi, Y. Kanesaki-Yatsuka, M. Matsumoto, Y. Mizuno, Y. Okazaki, Fam57b (Family with sequence similarity 57, member B), a novel peroxisome proliferator-activated receptor y target gene that regulates adipogenesis through ceramide synthesis. *J. Biol. Chem.* **288**, 4522–4537 (2013).
170. D. L. Tomasello, J. L. Kim, Y. Khodour, J. M. McCammon, M. Mitalipova, R. Jaenisch, A. H. Futerman, H. Sive, 16pdel lipid changes in iPSC-derived neurons and function of FAM57B in lipid metabolism and synaptogenesis. *iScience*. **25**, 103551 (2022).
171. S. Tanaka, T. Miyagi, E. Dohi, T. Seki, I. Hide, Y. Sotomaru, Y. Saeki, E. Antonio Chiocca, M. Matsumoto, N. Sakai, Developmental expression of GPR3 in rodent cerebellar granule neurons is associated with cell survival and protects neurons from various apoptotic stimuli. *Neurobiol. Dis.* **68**, 215–227 (2014).
172. Y. Huang, A. Skwarek-Maruszewska, K. Horré, E. Vandewyer, L. Wolfs, A. Snellinx, T. Saito, E. Radaelli, N. Corthout, J. Colombelli, A. C. Lo, L. Van Aerschot, Z. Callaerts-Vegh, D. Trabzuni, K. Bossers, J. Verhaagen, M. Ryten, S. Munck, R. D'Hooge, D. F. Swaab, J. Hardy, T. C. Saido, B. De Strooper, A. Thathiah, Loss of GPR3 reduces the amyloid plaque burden and improves memory in Alzheimer's disease mouse models. *Sci. Transl. Med.* **7** (2015), doi:10.1126/scitranslmed.aab3492.
173. S. Chen, Y. Zhou, Y. Chen, J. Gu, Fastp: An ultra-fast all-in-one FASTQ preprocessor. *Bioinformatics*. **34**, i884–i890 (2018).
174. N. L. Bray, H. Pimentel, P. Melsted, L. Pachter, Near-optimal probabilistic RNA-seq quantification. *Nat. Biotechnol.* **34**, 525–527 (2016).

175. D. M. Emms, S. Kelly, OrthoFinder: Phylogenetic orthology inference for comparative genomics. *Genome Biol.* **20**, 1–14 (2019).
176. C. W. Dunn, F. Zapata, C. Munro, S. Siebert, A. Hejnol, Pairwise comparisons across species are problematic when analyzing functional genomic data. *Proc. Natl. Acad. Sci. U. S. A.* **115**, E409–E417 (2018).
177. S. Álvarez-Carretero, A. U. Tamuri, M. Battini, F. F. Nascimento, E. Carlisle, R. J. Asher, Z. Yang, P. C. J. Donoghue, M. dos Reis, A species-level timeline of mammal evolution integrating phylogenomic data. *Nature*. **602**, 263–267 (2022).
178. D. W. Huang, B. T. Sherman, R. A. Lempicki, Systematic and integrative analysis of large gene lists using DAVID bioinformatics resources. *Nat. Protoc.* **4**, 44–57 (2009).
179. L. G. Mengjun, TCseq: Time course sequencing data analysis. R package version 1.8.0., 1–8 (2019).
180. M. I. Love, W. Huber, S. Anders, Moderated estimation of fold change and dispersion for RNA-seq data with DESeq2. *Genome Biol.* **15**, 1–21 (2014).
181. Y. Benjamini, Y. Hochberg, Controlling the False Discovery Rate□: A Practical and Powerful Approach to Multiple Testing. *J. R. Stat. Soc.* **57**, 289–300 (1995).

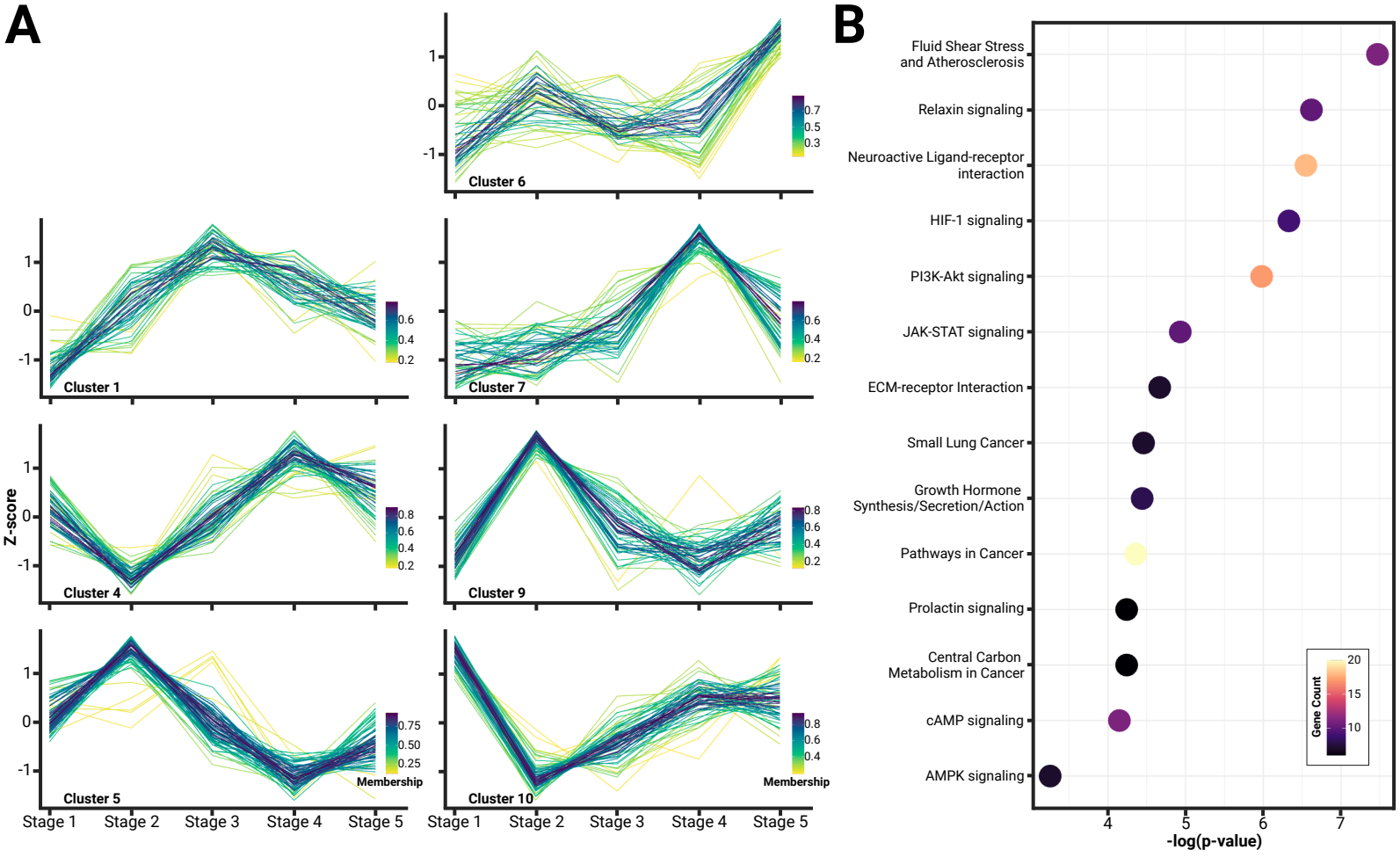
A
Cluster 1
Cluster 4
Cluster 5
Cluster 6
Cluster 7
Cluster 9
Cluster 10
Z-score
Membership
Stage 1
Stage 2
Stage 3
Stage 4
Stage 5
B
Fluid Shear Stress and Atherosclerosis
Relaxin signaling
Neuroactive Ligand-receptor interaction
HIF-1 signaling
PI3K-Akt signaling
JAK-STAT signaling
ECM-receptor Interaction
Small Lung Cancer
Growth Hormone Synthesis/Secretion/Action
Pathways in Cancer
Prolactin signaling
Central Carbon Metabolism in Cancer
cAMP signaling
AMPK signaling
Gene Count
-log(p-value)

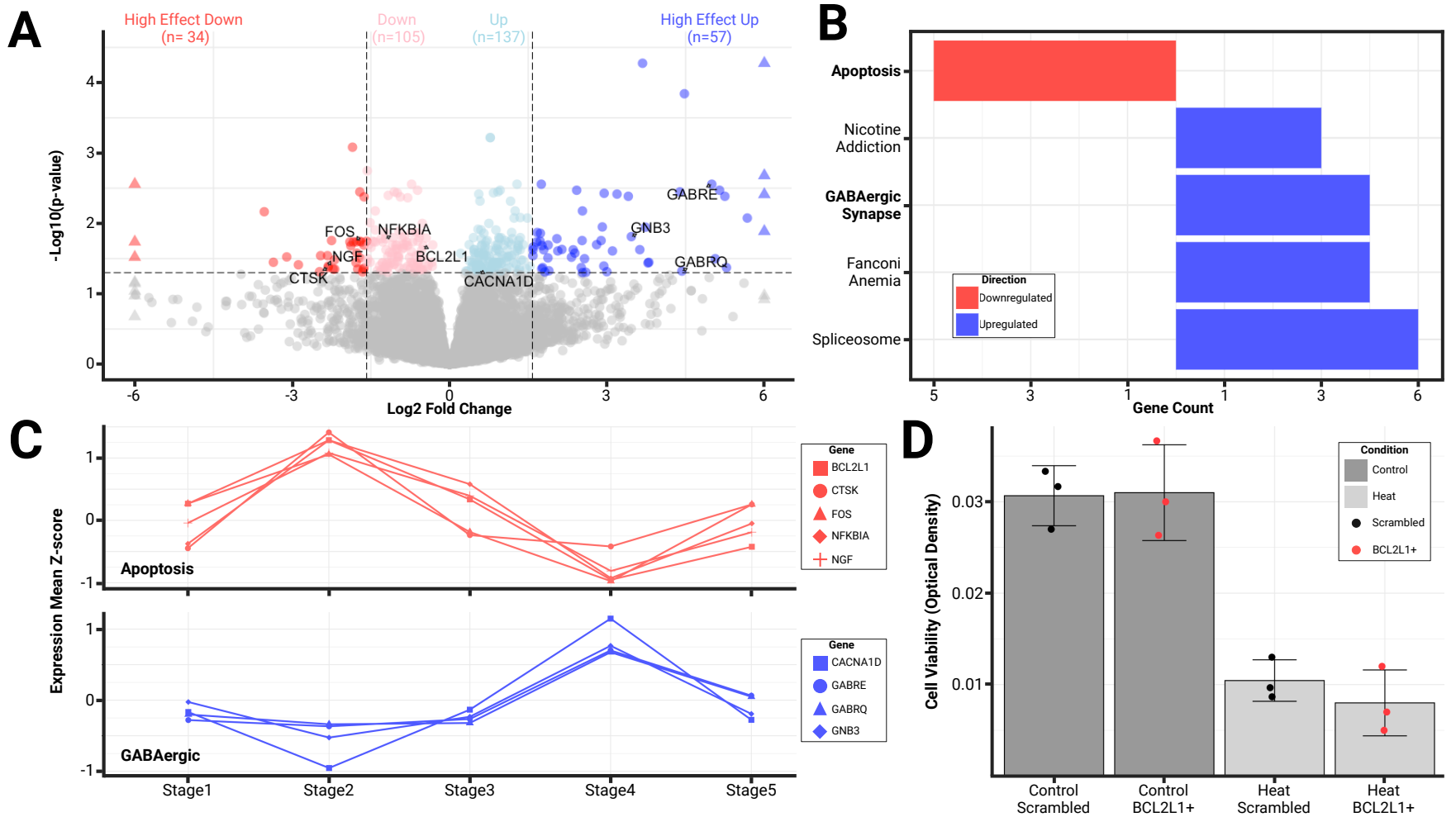
A
High Effect Down
(n= 34)
Down
(n=105)
Up
(n=137)
High Effect Up
(n=57)
-Log10(p-value)
Log2 Fold Change
FOS
NFKBIA
NGF
BCL2L1
CTSK
CACNA1D
GABRE
GNB3
GABRQ
B
Apoptosis
Nicotine Addiction
GABAergic Synapse
Fanconi Anemia
Spliceosome
Direction
Downregulated
Upregulated
Gene Count
C
Expression Mean Z-score
Apoptosis
GABAergic
Gene
BCL2L1
CTSK
FOS
NFKBIA
NGF
CACNA1D
GABRE
GABRQ
GNB3
Stage1
Stage2
Stage3
Stage4
Stage5
D
Cell Viability (Optical Density)
Condition
Control
Heat
Scrambled
BCL2L1+
Control Scrambled
Control BCL2L1+
Heat Scrambled
Heat BCL2L1+

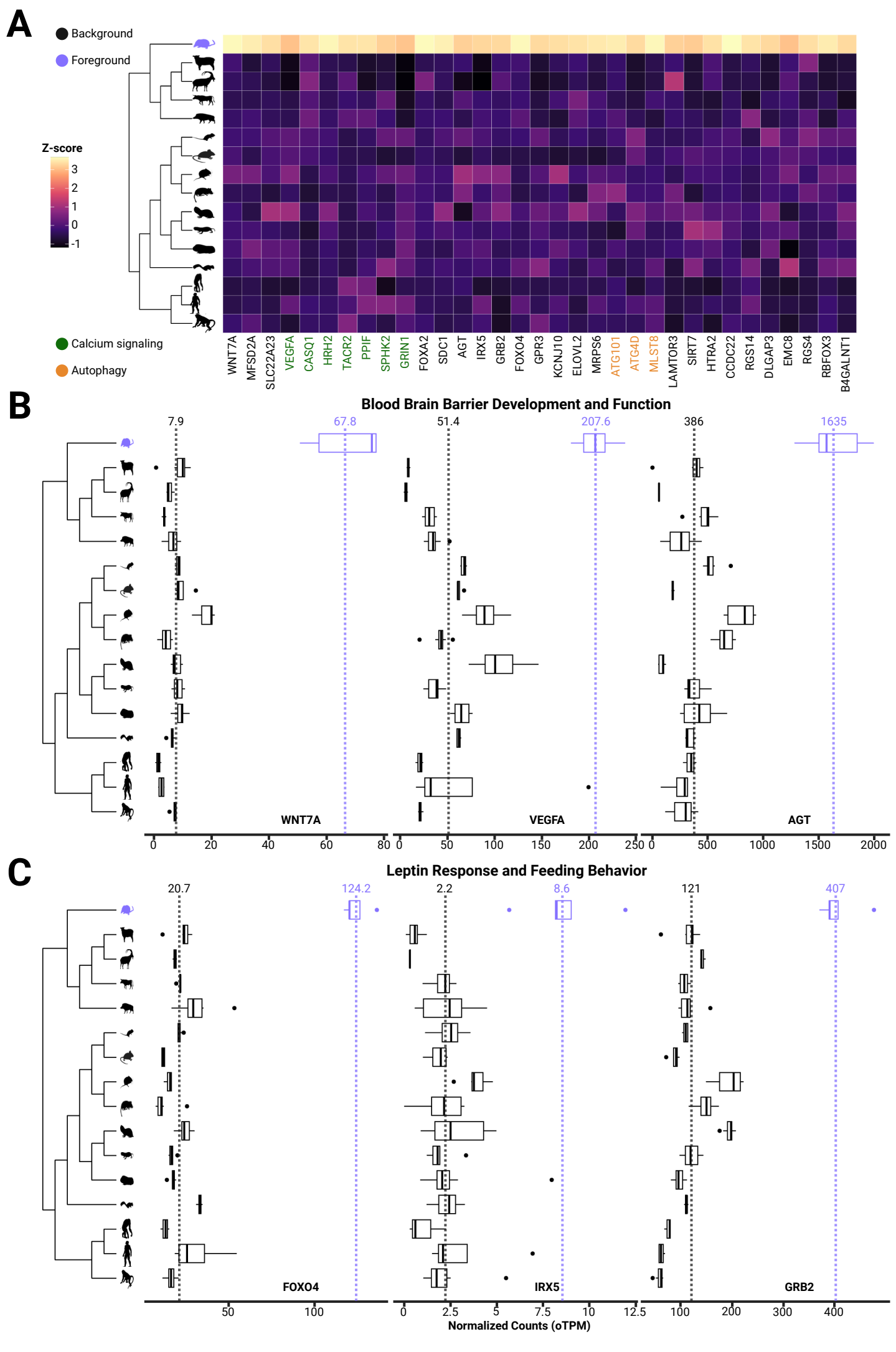
A
Background
Foreground
Z-score
3
2
1
0
-1
Calcium signaling
Autophagy
WNT7A
MFSD2A
SLC22A23
VEGFA
CASQ1
HRH2
TACR2
PPIF
SPHK2
GRIN1
FOXA2
SDC1
AGT
IRX5
GRB2
FOXO4
GPR3
KCNJ10
ELOVL2
MRPS6
ATG101
ATG4D
MLST8
LAMTOR3
SIRT7
HTRA2
CCDC22
RGS14
DLGAP3
EMC8
RGS4
RBFOX3
B4GALNT1
B
Blood Brain Barrier Development and Function
7.9
67.8
51.4
207.6
386
1635
WNT7A
VEGFA
AGT
0
20
40
60
80
0
50
100
150
200
250
0
500
1000
1500
2000
C
Leptin Response and Feeding Behavior
20.7
124.2
2.2
8.6
121
407
FOXO4
IRX5
GRB2
50
100
0
2.5
5
7.5
10
12.5
100
200
300
400
Normalized Counts (oTPM)

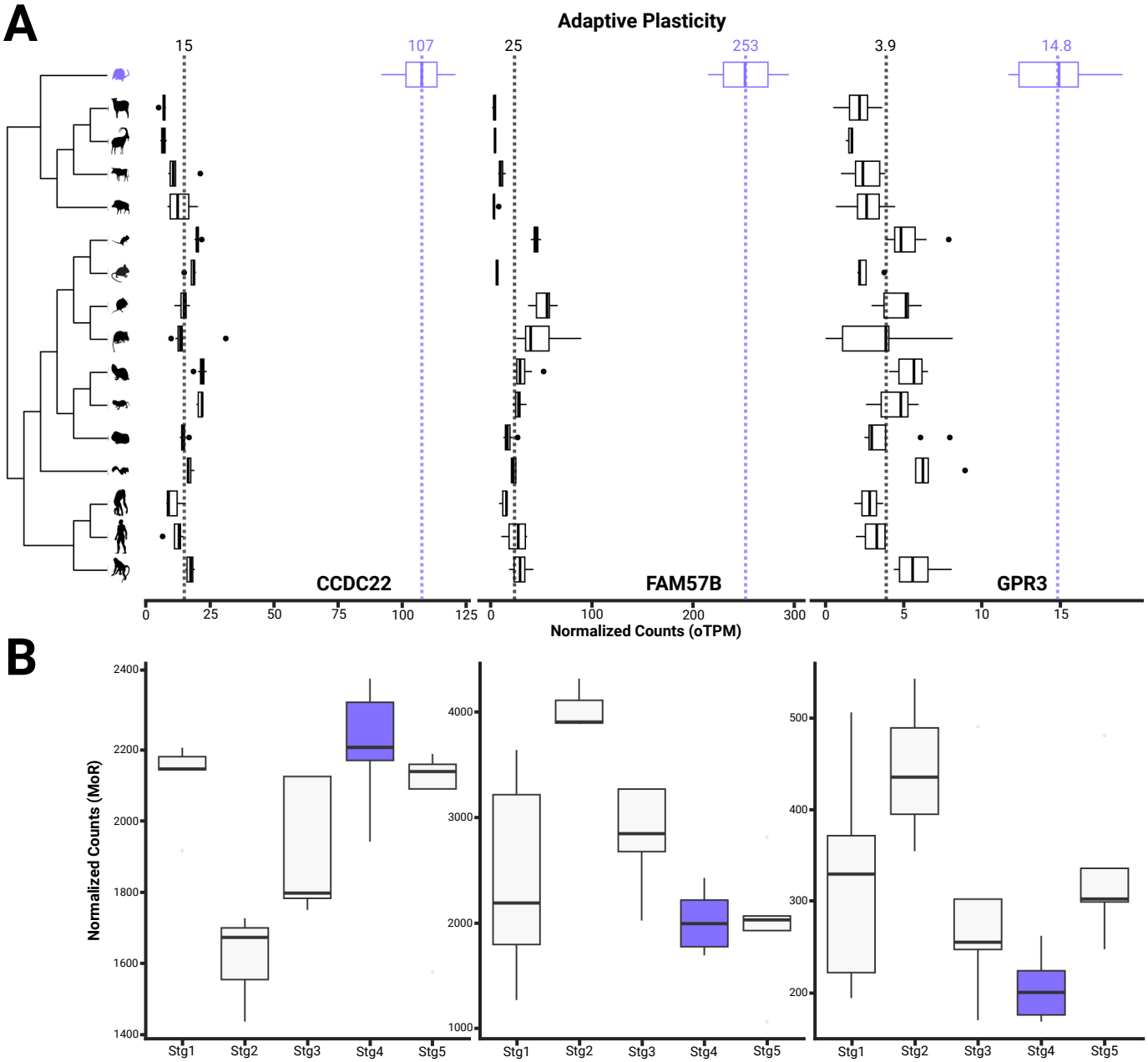
A
Adaptive Plasticity
15
107
25
253
3.9
14.8
CCDC22
FAM57B
GPR3
0
25
50
75
100
125
0
100
200
300
0
5
10
15
Normalized Counts (oTPM)
B
Normalized Counts (MoR)
2400
2200
2000
1800
1600
1400
4000
3000
2000
1000
500
400
300
200
Stg1
Stg2
Stg3
Stg4
Stg5